

Engineering SiO₂ Nanoparticles: A Perspective on Chemical Mechanical Planarization Slurry for Advanced Semiconductor Processing[†]

Ganggyu Lee^{1§}, Kangchun Lee^{2§}, Seho Sun^{3§}, Taeseup Song^{1*} and Ungyu Paik^{1*}

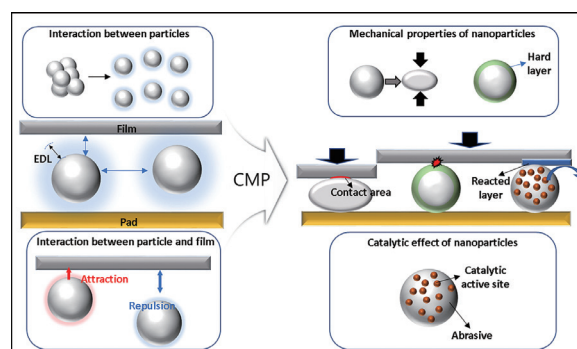
¹ Department of Energy Engineering, Hanyang University, Republic of Korea

² Department of Electronic Engineering, Kyonggi University, Republic of Korea

³ School of Chemical Engineering, Yeungnam University, Republic of Korea

Chemical mechanical polishing (CMP) is a process that uses mechanical abrasive particles and chemical interaction in slurry to remove materials from the surface of films. With advancements in semiconductor device technology applying various materials and structures, SiO₂ (silica) nanoparticles are the most chosen abrasives in CMP slurries. Therefore, understanding and developing silica nanoparticles are crucial for achieving CMP performance, such as removal rates, selectivity, decreasing defects, and high uniformity and flatness. However, despite the abundance of reviews on silica nanoparticles, there is a notable gap in the literature addressing their role as abrasives in CMP slurries. This review offers an in-depth exploration of silica nanoparticle synthesis and modification methods detailing their impact on nanoparticle characteristics and CMP performance. Further, we also address the unique properties of silica nanoparticles, such as hardness, size distribution, and surface properties, and the significant contribution of silica nanoparticles to CMP results. This review is expected to interest researchers and practitioners in semiconductor manufacturing and materials science.

Keywords: CMP (Chemical mechanical polishing), silica nanoparticles, synthesis, modification, surface functionalization, core-shell structure



1. Introduction

Chemical mechanical polishing (CMP) is a technique employed in the semiconductor fabrication process to remove material from the surface of films during integrated circuit (IC) manufacturing (Lee et al., 2022; Paik U. and Park J.-G., 2009). The process involves a chemical slurry and mechanical polishing by abrasive nanoparticles to achieve high planarity and smoothness on the film surface (Ein-Eli and Starosvetsky, 2007; Lee et al., 2016). IBM first developed and commercialized CMP in the late 1980s to planarize layers of silicon dioxide (SiO₂) during the fabrication of microelectronics (Beyer, 2015; Fury, 1997). CMP has attracted attention as a key step in manufacturing integrated circuits, including microprocessors, memory, and logic devices, due to growing demand for higher integration densities and smaller device sizes, which require

greater control over surface topography (Zwicker, 2022).

Fig. 1 illustrates the CMP process and the role of nanoparticles in CMP slurry (Mikhaylichenko, 2018; Seo, 2021). A multiple platen design offers flexibility in pad materials, slurries, and conditioning processes, enabling high throughput and optimized polishing. Wafers are cleaned after CMP and transferred back to their boxes by a robotic arm. A slurry is applied to the polishing pad, and the wafer rotates on a custom CMP table, where mechanical and chemical actions remove imperfections. After several steps, the wafer becomes ultra-smooth and ready for subsequent fabrication stages (Srinivasan et al., 2015).

The slurry consists of stable suspensions of abrasive nanomaterials, such as Al₂O₃ (alumina), SiO₂ (silica), and CeO₂ (ceria), dispersed in water with prescribed chemicals (Armini et al., 2008; Feng et al., 2006; Parker, 2004). The choice of abrasive nanoparticles depends on the type of polishing required. Silica is an abundant, representative, and versatile particle that minimizes defects and scratches, improves planarity and uniformity, and increases removal rates and selectivity (Lee et al., 2015).

Interactions between particles in suspended media are related to dispersion stability of the particles. Agglomerated

[†] Received 31 May 2023; Accepted 2 August 2023
J-STAGE Advance published online 28 December 2023

[§] Authors contributed equally to this publication

* Corresponding author: Taeseup Song; Ungyu Paik;
Add: 222 Wangsimni-ro, Seoul 04763, Republic of Korea
E-mail: tssong@hanyang.ac.kr (T.S.); upaik@hanyang.ac.kr (U.P.)
TEL: +82-2-2220-0502

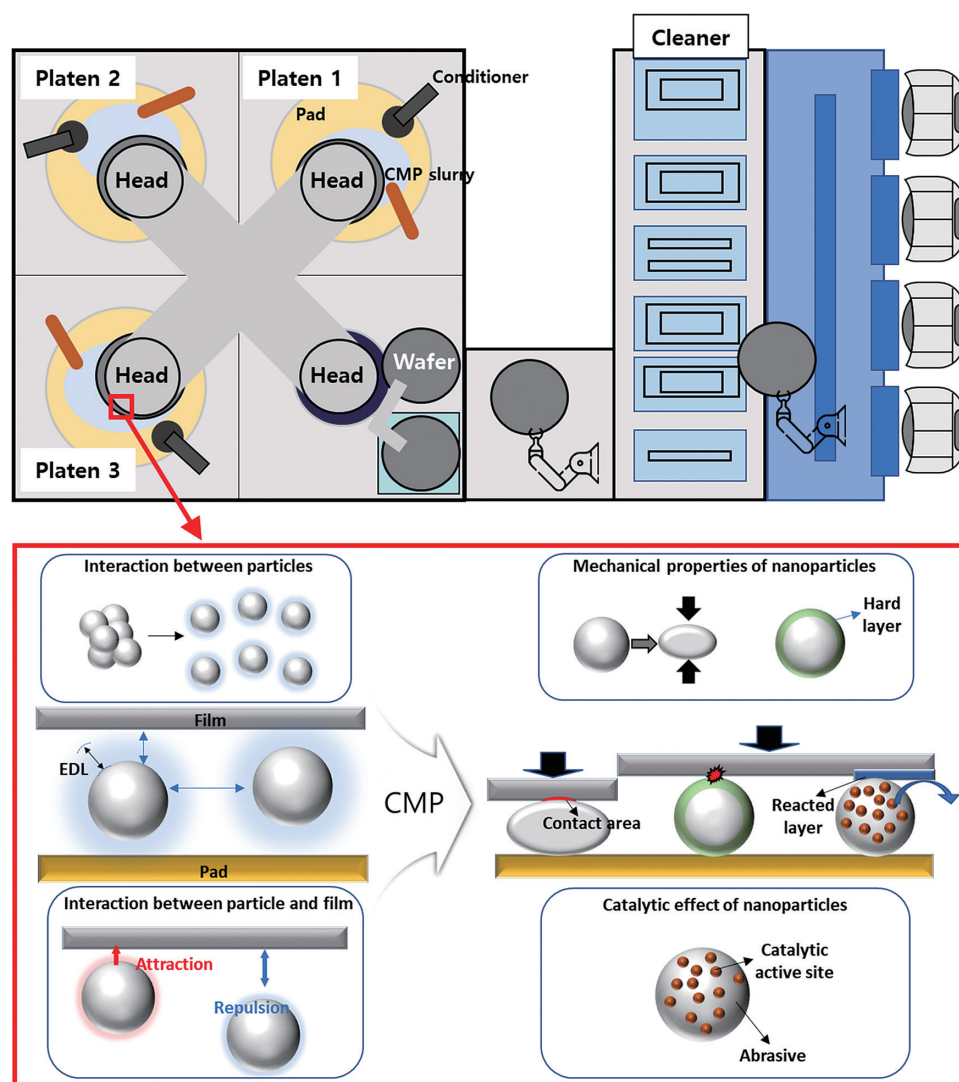


Fig. 1 Schematic illustrations of a standard CMP tool highlighting the influence of nanoparticle properties in the slurry on the CMP process. Key factors, such as the dispersion stability of nanoparticle abrasives in the slurry, interactions between particles and the film, the nanoparticle's elastic modulus and hardness, as well as their catalytic effects, are illustrated. These factors are crucial in determining the overall outcomes of CMP.

particles in CMP slurry can cause surface defects, reduce the CMP removal rate, and damage neighboring patterns, resulting in lower selection ratio. In particular, aggregate particles larger than 1 μm in diameter are a leading cause of scratch defects on films (Armini et al., 2008; Lu et al., 2013; Seipenbusch et al., 2010; Shin et al., 2019). Van der Waals and electrostatic forces are critical factors influencing the cohesion and stability of particles in suspended media. Van der Waals forces always act as an attractive force between particles, and a system dominated by van der Waals forces results in particle agglomeration. The electrostatic force that acts as a repulsive force between two particles is the electrostatic force. In the aqueous system, the adsorbed ions on the nanoparticles determine the repulsive force between the particles. Ions distributed around the nanoparticle form an electric double layer (EDL) (Hayashi et al., 1995). The Coulomb force produced by an EDL is an electrostatic and repulsive force between

particles of the same material; the thicker the EDL, the stronger the repulsive force between the particles and the weaker the agglomeration (Gun'ko et al., 1998). These forces can be controlled by adjusting the slurry chemistry, and nanoparticle engineering can help maintain a stable slurry, prevent particle agglomeration, and ensure a successful polishing process.

Material removal occurs when abrasive particles and the substrate surface are in direct contact (Luo and Dornfeld, 2003). Contact between abrasive particles and films also occurs when van der Waals and electrostatic forces dominate the attraction, resulting in higher removal rates. Controlling the attraction or repulsion between abrasive particles and the film surface is critical for improving removal rates and selectivity. A model based on the contact mechanism has been proposed to explain the mechanical aspects of the material removal mechanism (Seo et al., 2016b). According to the model, the greater the total

contact area between the particle and the film, the greater the removal rate. Assuming all particles participate in material removal, the particle-film surface contact area is calculated as $A \propto C^{1/3} \cdot d^{-1/3}$, where C is the concentration of abrasive particles, and d is the abrasive diameter (Basim et al., 2000). However, only abrasive particles larger than the gap between the polishing pad and the film surface (active particles) can contribute to material removal (Seo, 2021).

Another key property of nanoparticles can affect CMP performance. First, the catalytic effect of nanoparticles can improve the removal rate during metal CMP by enhancing the oxidation reaction (Lei et al., 2012; Wang et al., 2016). Second, the mechanical properties of the particles. The ability to control the elastic modulus can increase the removal rate by enlarging the contact area with the film and reducing scratches and roughness (Chen et al., 2019; Mu and Fu, 2012). Moreover, improving the abrasive surface hardness is advantageous for achieving higher removal rates, especially when working with films with relatively high hardness and chemical stability, such as alumina, silicon carbide (SiC), and tungsten (Dai et al., 2020). Therefore, careful selection and use of nanoparticles with these desirable properties can significantly impact the efficiency of CMP.

As the materials for the next generation of semiconductor devices become more diverse and the device structures more complex, the performance requirements for CMPs are becoming increasingly stringent. Silica nanoparticle abrasives, which can reduce defects and scratches, improve flatness and uniformity, and increase removal rates and selectivity, are among the most popular materials. This review of silica nanoparticles as CMP abrasives is organized in the following order: properties of nanoparticles that affect CMP, silica particle synthesis methods and their properties, and finally, silica nanoparticle modifications such as surface functionalization, coating or doping with other materials, and core-shell structure formation to overcome the limitations of conventional synthesis methods.

2. Nanoparticle properties and their impact on CMP

Nanoparticle abrasives in slurries can affect CMP results due to their dispersion stability, interactions between particles and film, elastic modulus and hardness, and catalytic effects (Fig. 1). Dispersion stability is closely related to interactions between nanoparticles (Kawaguchi, 2020). When there is a sufficient repulsive force between nanoparticles, dispersion stability increases. A slurry with high dispersion stability prevents scratch defects caused by agglomerated particles and contributes to improved planarity through uniform removal on the film surface and increased removal rates by enlarging the contact area (Choi et al., 2004). Interactions between particles and films affect the number of active particles (Wang et al., 2022). Increasing

the force between particles and films increases both the number of active particles and removal rate (Hwang et al., 2008). This is also important for selectivity control in patterned wafers (Seo et al., 2014). The elastic modulus and hardness of the particles are related to the removal rate and defects. Depending on the target film, particle design should consider whether the main issue is high defects or low removal rate (Kwon et al., 2013; Saka et al., 2008). The last catalytic effect refers to the effect of particles on the promotion of chemical reactions on the film surface (Wang et al., 2021). To improve the performance of CMP, it is necessary to understand and control these nanoparticle properties.

2.1 Interactions between nanoparticles in suspension

Between 1945 and 1948, two research teams, one led by Derjaguin and Landau in the Soviet Union and the other by Verwey and Overbeek in the Netherlands, independently proposed a theory regarding repulsion between charged particles in water (Ninham, 1999). This is now commonly referred to as the DLVO theory, after the initials of the four scientists involved (van Oss, 2008).

The DLVO theory suggests that the stability of a particle in solution depends on its total potential energy function (V_T). The primary potential energy between two particles arises from the attractive van der Waals force (V_A) and the electrostatic force (V_R) from the electrical double layer. An extended DLVO theory, which incorporates the steric force (V_S) due to adsorbed layers of polymers or surfactants, has been proposed to better explain the stabilization of colloidal systems (van Oss, 2008). This can be represented by the equation:

$$V_T = V_A + V_R + V_S \quad (1)$$

The van der Waals force is the attraction resulting from the instantaneous dipoles formed by temporary polarization of atoms and the induced dipoles caused by these instantaneous dipoles (Fig. 2(a)) (Mauguin, 1939). This force is always present in nanoparticles within a dispersion and becomes significantly stronger when the distance between particles decreases. The van der Waals force is a major reason for particle agglomeration. The equation for the van der Waals force between two spherical particles (Hamaker, 1937) can be expressed as

$$V_A(s) = -\frac{A}{3} \left[\frac{R^2}{s(s+4R)} + \frac{R^2}{(s+2R)^2} + \frac{1}{2} \ln \left(1 - \frac{4R^2}{(s+2R)^2} \right) \right] \quad (2)$$

$$V_A(s) = -\frac{AR}{12s} \quad (s \ll R) \quad (3)$$

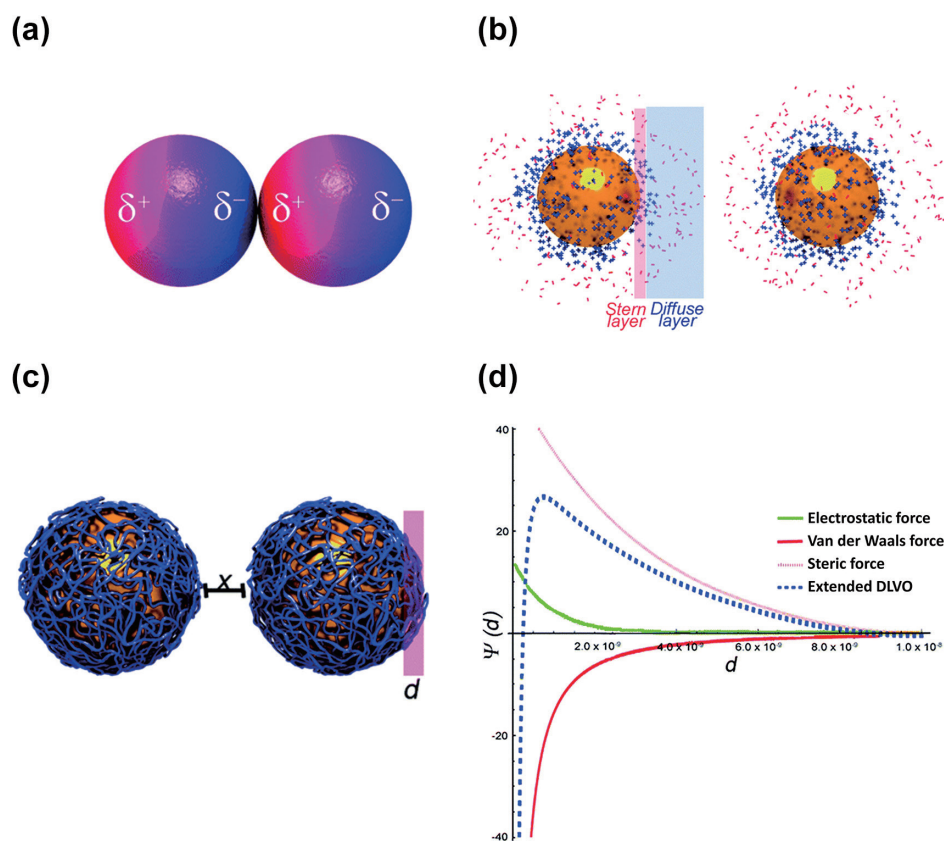


Fig. 2 Interactions between nanoparticles in CMP slurry according to DLVO theory: (a) van der Waals force, (b) electrostatic force, (c) steric force and (d) the potential as a function of the distance between two particles derived from their net potential. Reproduced from Ref. (Moore et al., 2015) with permission from the Royal Society of Chemistry.

where A is the Hamaker constant, s is the distance between the two particles, and R is the radius of the spherical particle. When the distance between two particles is small enough, as in Eqn. (3), the expression can be approximated. According to this equation, the larger are the particles, the shorter is the distance; and the higher is the Hamaker constant, the stronger is the van der Waals force. The Hamaker constant is determined by the dielectric constant and refractive index of the nanoparticles and the dispersion medium (Bergström, 1997). The Hamaker constant is difficult to manipulate once the materials of nanoparticles and medium are determined. Much research into increasing dispersion stability has been directed toward increasing the repulsive forces rather than reducing van der Waals forces (Tolias, 2018).

Charges on particle surfaces can influence electrostatic forces. In an aqueous system, nanoparticles acquire charges based on pH (Serrano-Lotina et al., 2023). In acidic conditions, they carry a positive charge, which gradually weakens as the pH increases, and they carry a negative charge in alkaline conditions. A surface charge occurs because protons adsorb and bind to a particle surface under acidic conditions, generating a positive charge. A negative charge arises as the pH increases and hydroxide ions become more prevalent. In other words, the degree of surface charge depends on the reactivity with protons or hydroxide ions.

When a particle acquires a surface charge by binding with a proton or hydroxide ion, counter ions are adsorbed to the exterior, forming an EDL, which consists of a Stern layer (the first layer strongly bound to the particle surface) and a diffusion layer outside of which ions are distributed (Fig. 2(b)). The two layers differ because the potential linearly decreases with distance in the Stern layer, where the particles are strongly bound (Lunardi et al., 2021). In contrast, in the diffusion layer, the effects of surface charge and thermal motion are considered together, resulting in parabolic potential behavior.

Each material has a pH at which the charge becomes zero, called the isoelectric point (IEP) (Seo et al., 2016a). The IEP varies by material, and it is important to understand the IEP of each material and to select a pH that maintains sufficient electrostatic repulsive force. For example, pure silica typically has an IEP of 2 to 3, and alumina has an IEP of 9 (Kosmulski, 2009). The IEP is inversely proportional to the electronegativity of the metal composing the oxide, with a higher electronegativity leading to a lower IEP (Bebieet al., 1998). Factors affecting IEP also include particle functional group and crystal facet number and impurity.

The steric force between particles is caused by the adsorption of polymers (Fig. 2(c)). Steric forces can be largely divided into the force for volume restriction (ΔG^{VR})

and the force by mixing energy (ΔG^M). The former represents the repulsive force caused by the volume of the polymer, while the latter is caused by osmotic pressure due to the affinity between the solvent and the polymer as the polymer layers approach each other (Sedev and Exerowa, 1999). When the adsorbed particles of the two polymers are separated by less than the distance between the polymer layers, a force due to ΔG^M is generated. At this point, the relationship between the polymer and the solvent is important. In an effective solvent with a strong affinity between the polymer and the solvent, the solvent penetrates by osmotic pressure and causes a repulsive force (Babchin and Schramm, 2012). When the two particles approach each other, a repulsive force is generated by ΔG^{VR} .

The interaction between two particles, depicted in Fig. 2(d), is determined by the combined forces of van der Waals forces, the electrostatic force due to the EDL, and steric forces. If this value is positive, repulsive forces dominate, resulting in higher dispersion stability. If it is negative, attractive forces dominate, and the particles agglomerate (Moore et al., 2015).

2.2 Interactions between nanoparticles and film during CMP

When nanoparticles and film substrates interact in an aqueous system, the adhesion between them is influenced by van der Waals, electrostatic, and steric forces. These forces can either attract or repel particles from the surface, affecting the rate of removal. Measuring these forces directly can be difficult, but atomic force microscopy (AFM) can now gauge the net force between the particles and substrate (Kappl and Butt, 2002). AFM is a powerful tool in various research fields, including powder technology. It uses a probe with a sharp tip to scan the surface of a sample and detect the reflected laser beam to create an image (Shluger et al., 1994). An AFM instrument has a basic configuration, consisting of a micro-machined cantilever with a sharp tip, a piezoelectric scanner, and a photodiode detector (Fig. 3(a)). AFM can also be performed in liquid environments using a fluid cell (Dorobantu et al., 2009).

To apply AFM to force measurement, the probe or sample substrate is moved vertically (z-direction) to change the distance between the probe and the surface (Kappl and Butt, 2002). By attaching a colloidal nanoparticle at the end

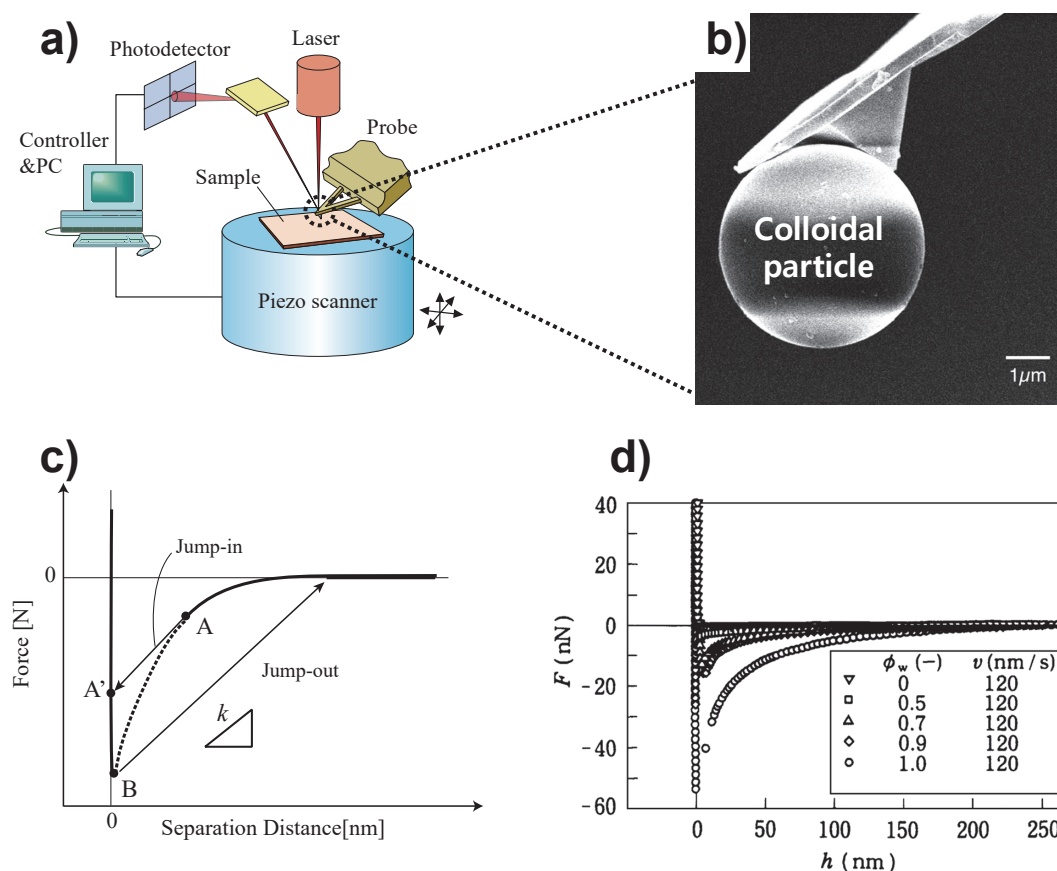


Fig. 3 Analysis of particle-film interactions through force-distance curve measurements by AFM: (a) schematic of AFM equipment, (b) an AFM cantilever with colloidal particles attached, (c) force-distance curve measurement results using an AFM cantilever with colloidal particles attached, and (d) surface charge variation with the ratio of water and IPA and corresponding force distance curve variation. Reusing with permission from Ref. (Ishida and Craig, 2019) under the terms of the CC-BY 4.0 license. Copyright: (2019) The Authors, published by Hosokawa Powder Technology Foundation.

of the pointed tip, the force-displacement curve between the particle and substrate can be obtained. For colloidal probes (**Fig. 3(b)**), spherical particles between 2 μm and 40 μm in diameter are typically attached to the probe with an epoxy adhesive or hot-melt epoxy resin (Ralston et al., 2005).

For the force in **Fig. 3(c)**, the attraction between the surfaces is sensed. When the surfaces are in contact, the change in cantilever deflection is equal to the change in displacement, often represented by a linear region called the constant compliance region (Ishida and Craig, 2019). It is necessary to focus on the shape of the curve, which suddenly decreases or increases before re-entering the constant compliance region (**Fig. 3(d)**). When attraction is a strong function of separation, the instability of the cantilever often causes the surfaces to “jump in” to a contact (denoted by A and A' in **Fig. 3(c)**). This occurs when the gradient of the interaction force with separation distance exceeds the spring constant of the cantilever. As the surfaces separate, adhesion may appear between them. In this case, the cantilever typically “jumps out” with zero interaction force, as represented by point B in the figure. This is the opposite effect of jumping in. If the system were applied to a repulsive force, the curve would instead bend to a positive value first before reaching the compliance region.

2.3 Mechanical properties of nanoparticles

AFM nano-indentation is an effective method to deter-

mine the elastic behavior of samples by analyzing force-displacement curves and nano-indentation data. Passeri et al. (2011) used AFM to measure the elastic modulus (E) and hardness of polyaniline films on glass substrates. Nowatzki et al. (2008) computed the E values of thin films using the thin-film Hertzian model. Song et al. (2008) assessed the E values of PS, polymethylmethacrylate (PMMA) spheres, and PMMA/silica composites by applying an AFM force-volume technique and Hertz's theory of contact mechanics (**Table 1**) (Chen et al., 2015a).

In AFM indentation tests, the shape of the indenter (cantilever tip) significantly influenced the calculated results. Indenters can be modeled in two geometries: spherical or conical (depicted in **Fig. 4(a)** and **(b)**). **Eqns. (4)** and **(5)**, which are related to force, indentation, and Young's modulus, were utilized to compute the results, where F represents the indentation force, δ denotes the indentation depth, R is the tip radius, and α is the half-opening angle of the conical tip. The reduced modulus of elasticity (E^*) can be calculated using E and ν for the sample and E_t and ν_t for the AFM tip, as shown in **Eqn. (6)**. If the elastic modulus of the indenter is much greater than that of the sample, E^* can be simplified, as shown in **Eqn. (7)** (Chen et al., 2015a).

$$F_{\text{Sphere}} = \frac{4}{3} \cdot E^* \cdot \delta^{3/2} \cdot R^{1/2} \quad (4)$$

$$F_{\text{Cone}} = \frac{2}{\pi} \cdot E^* \cdot \delta^2 \cdot \tan(\alpha) \quad (5)$$

Table 1 Core shell structure mechanical properties by the composition of particles. Reprinted with permission (Chen et al., 2015a). Copyright: (2015) Elsevier B.V.

Samples	Core size [nm]	Shell thickness [nm]	E [GPa]
PS	200	—	2.01 ± 0.70
PS/SiO ₂	200	10	4.42 ± 0.27
PS/SiO ₂	200	15	5.88 ± 0.48
PS/SiO ₂	200	20	9.07 ± 0.94
PS	120	—	2.80
PS/CeO ₂	120	8	7.93
PS	120	12	8.25
PS	120	16	10.67
PMMA	367	—	4.3 ± 0.7
PMMA/SiO ₂	367	15	4.5 ± 0.7
PMMA/SiO ₂	367	30	10.3 ± 1.5
PP	200–500	—	1.3–2.8
Bulk PP	—	—	1.5–2.0
Bulk PS	—	—	2–5
Bulk SiO ₂	—	—	75, 72
Bulk CeO ₂	—	—	264.1

$$\frac{1}{E^*} = \frac{1-\nu^2}{E} + \frac{1-\nu_t^2}{E_t} \quad (6)$$

$$\frac{1}{E^*} \approx \frac{1-\nu^2}{E} \quad (7)$$

Chen et al. (2015a) conducted experiments by depositing particles through spin coating on the substrate (Fig. 4(c)). They measured the modulus of the particles by contacting the tip at the location where the particle was located and measuring the F value according to the depth of indentation. Fig. 4(d) shows the force-distance curve of a spin-coated deposit of nanoparticles on a substrate. Retract curve was fitted using the Hertzian model (using a spherical indenter), and as shown in this figure, the fitted curve was mainly consistent with the force-distance curve. This fitting allowed us to measure the elastic modulus of the nanoparticle using the force-distance curve.

There are several possible sources of error in calculating the elastic modulus, such as uncertainty in contact point determination and errors in k_c measurement of AFM cantilevers, surface and probe roughness, scanner and sample creep, and AFM photodetectors. Chen et al. (2015a) found that the substrate can also influence the measured mechanical properties, causing some error in the results. Despite

these sources of error, it is possible to measure the relative change in modulus for each particle under the same measurement conditions.

2.4 Catalytic effect of nanoparticles

Kauffman proposed a model for CMP of tungsten and similar metals, in which the surface is oxidized to form a weak interface between the metal oxide and the metal (Lim et al., 2013; Tamboli et al., 1999). The abrasive attacks the weak interface to remove material. This model has been applied not only to tungsten, but also to metals such as copper, cobalt, and molybdenum, as well as materials with high hardness, including sapphire and SiC, to secure an adequate removal rate during polishing (Krishnan et al., 2010).

To promote oxidation reactions on the surface of the material being polished, catalysts and oxidizing agents are essential. Metals (Ag, Fe) and metal oxides such as copper oxide (CuO, Cu₂O), silver oxide (Ag₂O), and iron oxide (Fe₂O₃, Fe₃O₄) can act as catalysts in the reaction that decomposes the most commonly used CMP oxidizing agent, H₂O₂, to produce hydroxyl (OH) radicals (Kanungo, 1979; Xu et al., 2014). However, these particles do not ensure

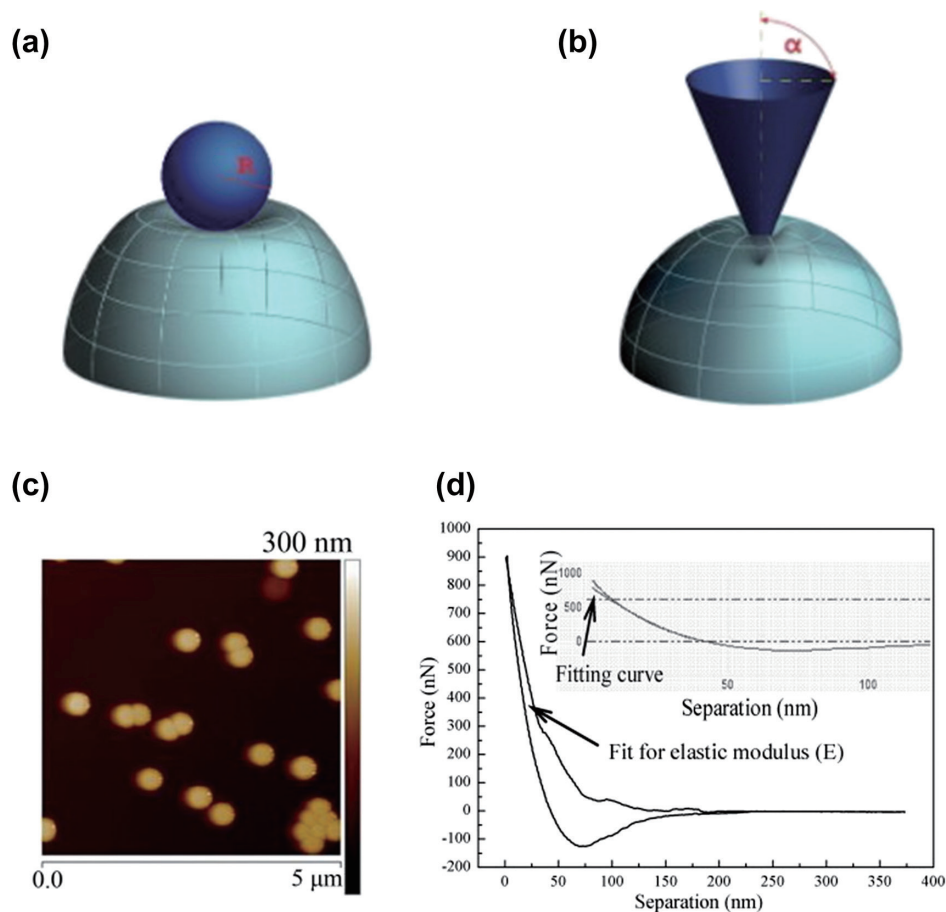


Fig. 4 Measurement of mechanical properties through force-distance curve measurements by AFM: Tip-particle surface contact models: (a) spherical indenter and (b) conical indenter. (c) AFM 2D image of nanoparticles deposited on the substrate. (d) Force separation curves and fitting curves obtained from nanoparticles. Reprinted with permission from Ref. (Chen et al., 2015a). Copyright: (2015) Elsevier B.V.

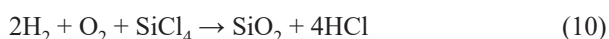
dispersion stability or achieve desirable polishing rates from a mechanical perspective (Guedes et al., 2009; Xu et al., 1998). Commonly used CMP abrasives such as silica, alumina, and ceria do not have any catalytic effects on oxidation reactions. Research on the use of composites of catalyst-containing particles and abrasives in CMP will be discussed in detail later.

3. Synthesis strategy for silica nanoparticles to improve CMP

The choice of abrasive plays a crucial role in the performance of a CMP slurry, as slurry properties can vary widely depending on the synthesis method. Silica particles, which are a common component of CMP slurries, can be classified into two types: fumed silica, which is synthesized through a gas phase process, and Stöber (or colloidal) silica, which is synthesized through a liquid phase process (Hyde et al., 2016). Table 2 outlines the advantages and disadvantages of each type. Fumed silica offers a large surface area and an amorphous structure, but its irregular shape and wide particle-size distribution can lead to surface defects during polishing (Khan et al., 2004). By comparison, Stöber silica with uniform particle size and shape can result in more predictable polishing and fewer surface defects (Ahn et al., 2004). However, its lower removal rate compared to fumed silica is still an issue that needs to be overcome (Kim et al., 2021). Ultimately, the choice between fumed and Stöber silica depends on the specific requirements of the CMP, which may include desired material removal rate, selectivity, surface finish, and slurry stability.

3.1 Gas phase synthesis: fumed silica

Flame hydrolysis is a large-scale industrial process that generates silica with large surface area. Fig. 5(a) illustrates the flame hydrolysis setup for producing fumed silica. The synthesis reaction equations follow (Garrett, 2017; Hyde et al., 2016);



Fumed silica is synthesized by combusting silicon tetrachloride (SiCl_4) or other silicon-containing precursors in a hydrogen-oxygen flame (Khavryutchenko et al., 2001). The heat from combustion vaporizes the SiCl_4 , which then reacts with water vapor to form silica nanoparticles.

These primary particles coagulate through intergrowth in the flame and agglomerate due to cohesive forces during and after cooling. Silica is separated from the off-gas containing hydrogen chloride (HCl) using filters or cyclones. The high-temperature residence time, along with the interplay of surface growth, coagulation, and sintering, determines the characteristics of the particles. These nanoparticles aggregate into chains and ultimately form a three-dimensional network structure, resulting in fumed silica (Fig. 5(b)) (Jin et al., 2019; Meled, 2011).

Fumed silica nanoparticles are an anhydrous material synthesized using gas-based dry processes, resulting in low concentration of surface silanol (Si-OH) groups. When silica nanoparticles are dispersed in aqueous solutions, the silanol groups on their surface can form hydrogen bonds with water molecules and develop a surface charge through reactions with H^+ or OH^- ions, which are potential determining ions. These reactions are the driving force for the good dispersion of nanoparticles. However, fumed silica can be challenging to disperse in water, and the rheological properties of the dispersion exhibit shear thinning behavior (Barthel et al., 2005; Kim et al., 2021; Liu and Maciel, 1996). In static condition, the silanol groups on the surface interact weakly with fluids through hydrogen bonding, increasing the viscosity of the fluid. In dynamic environment, even mild shear deformation can break the connection between fluid molecules and silica due to the relatively small number of silanol groups available for hydrogen bonding. This is a characteristic observed in fumed silica dispersions due to shear thinning, a decrease in viscosity under shear stress.

Table 3 lists the results of CMP on SiO_2 layer using fumed silica-based slurry. The data indicate that the removal rate increased as the particle size grew from 80.2 to 138 nm (Kim et al., 2021). The increase in removal rate is due to the more frequent and direct interaction of the larger particles with the film surface and the larger penetration

Table 2 Comparing the advantages and disadvantages of fumed silica and Stöber silica aspect to the CMP process.

	Fumed silica	Stöber silica
Advantages	<ul style="list-style-type: none"> • Easy for mass production • High purity • Large surface area to volume • High removal rate 	<ul style="list-style-type: none"> • Monodisperse size distribution • Regular and spherical particle shape • High dispersion stability • Lower surface defects and scratches
Disadvantages	<ul style="list-style-type: none"> • Wide size distribution • Irregular shape of the particle • Difficult to control secondary particle size and dispersion stability • Causing surface defects and scratches 	<ul style="list-style-type: none"> • Expensive precursor price • Alcohol by-product • Low removal rate • Small surface area to volume

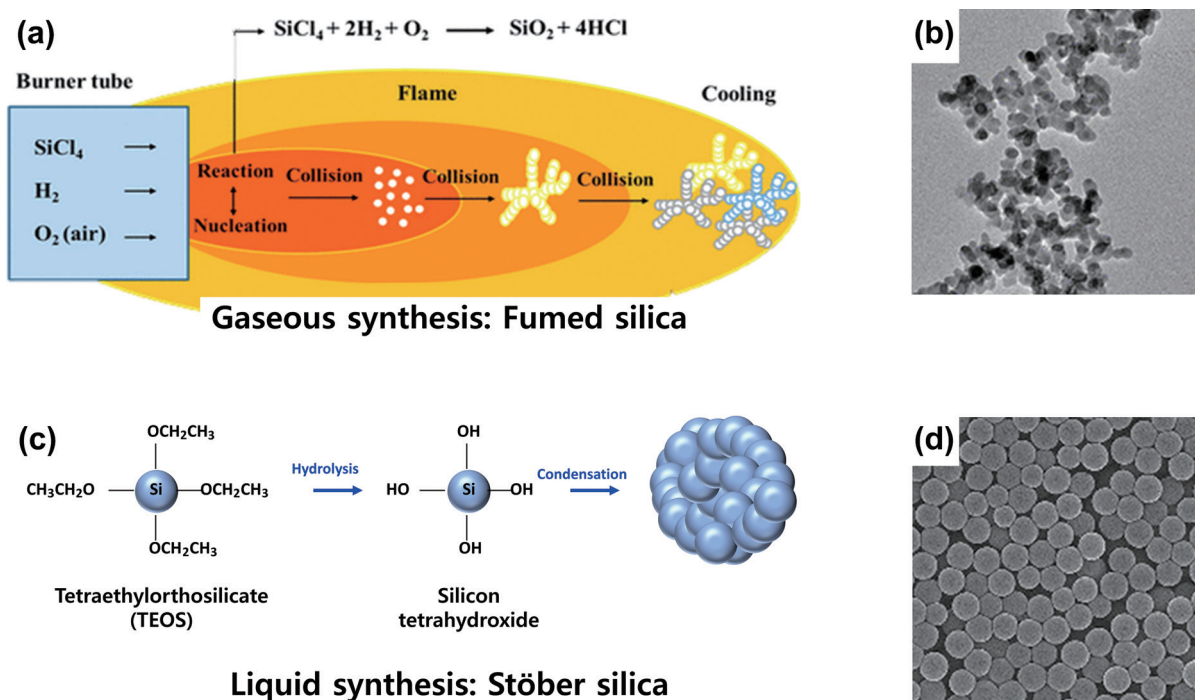


Fig. 5 (a) Schematic illustrations of fumed silica nanoparticle synthesis through gas-phase reaction for CMP slurry. Reprinted with permission (Hyde et al., 2016). Copyright: (2016) American Chemical Society. (b) TEM images displaying the morphologies of the fumed silica nanoparticles. Reprinted with permission from (Chen et al., 2022). Copyright: (2022) American Chemical Society. (c) Schematic illustrations of Stöber silica nanoparticle synthesis through liquid-phase reaction for CMP slurry. (d) TEM images displaying the morphologies of Stöber silica nanoparticles. Reprinted from Ref. (Sui et al., 2016) under the terms of the CC-BY 4.0 license. Copyright: (2016) The Authors, published by Springer Nature.

Table 3 CMP results using fumed silica-based slurry.

Size [nm]	Solid loading [%]	pH (Adjustor)	CMP pad	Applied pressure [psi]	Removal rate [Å/min]	Roughness [nm]	Reference
140.9	12	10.5 (NH ₄ OH)	IC1000/subaIV	4	2600	Ra 0.29	(Kim et al., 2021)
138.8	12	10.5 (NH ₄ OH)	IC1000/subaIV	4	2850	Ra 0.31	(Kim et al., 2021)
99.4	12	10.5 (NH ₄ OH)	IC1000/subaIV	4	1500	Ra 0.17	(Kim et al., 2021)
80.2	12	10.5 (NH ₄ OH)	IC1000/subaIV	4	1200	Ra 0.14	(Kim et al., 2021)
156	10	10.5 (NH ₄ OH)	IC1400	4	1680	RMS 0.25	(Haba et al., 2003)
220	15	10.1 (KOH)	IC1000/subaIV	3	620	—	(Estel et al., 2010)
220	15	4.1 (HCl)	IC1000/subaIV	3	80	—	(Estel et al., 2010)
220	15	3.0 (HCl)	IC1000/subaIV	3	10	—	(Estel et al., 2010)

volume. However, as the particle size exceeded 138 nm, the contact area decreased, gradually decreasing the removal rate (Haba et al., 2003). That means the contact area becomes more dominant in the removal rate above a specific particle size than the penetration volume. Whether the penetration volume or contact area is the dominant factor in

the removal rate depends on the film and particle being polished and the process conditions (Basim et al., 2000). As shown in Table 3, for CMP of SiO₂ layer with fumed silica, the contact area or penetration volume becomes the more important factor starting from 138 nm. Below 138 nm, the effect of the penetration volume is more dominant on the

removal rate change, and above 138 nm, the contact area is more dominant. However, CMP with particles penetrating the film can cause many defects in the post-CMP film, which is why the roughness increases with increasing size up to 138 nm.

Fumed silica needs adequate electrostatic repulsive force for effective dispersion (Estel et al., 2010). Due to its low ion impurity content, the IEP of fumed silica falls between pH 2 and 3. As a result, fumed silica demonstrated high dispersion stability at pH 10, where the surface charge is high, but poor dispersion stability near its IEP at pH 3. This led to a high removal rate at pH 10, which can be attributed to the greater contact area between particles and the film substrate. In contrast, a low removal rate was observed at pH 4 due to the reduced dispersion stability.

Fumed silica offers several advantages, such as the ability to be synthesized in large-scale processes to high purity levels due to its nearly complete absence of ionic impurities, as well as the high hardness of the primary particles with few pores. In the early days of implementing CMP in semiconductor manufacturing processes, fumed silica-based CMP slurries were widely used, particularly for interlayer dielectric CMP, to remove the SiO₂ layer (Li et al., 2010). However, excessive energy requirements and harsh reaction conditions, which produce toxic gases such as hydrogen chloride (HCl), reduced its usefulness in efficiency-minded and environmentally conscious societies (Croissant et al., 2020). Moreover, as semiconductor devices become ever smaller, the standards for defects and scratches are becoming more stringent. In conclusion, the shift from fumed silica to Stöber silica in CMP slurries for semiconductor manufacturing reflects the industry's increasing focus on environmental sustainability, energy efficiency, and the need for high-quality materials with better control over particle size, shape, and dispersion stability to meet the demands of ever-shrinking electronic devices.

3.2 Liquid phase synthesis: Stöber silica

The Stöber method named after Werner Stöber, is a sol-gel process for synthesizing monodisperse spherical silica nanoparticles (Ibrahim et al., 2010). The method involves hydrolyzing and condensing alkoxysilane precursors such as tetraethyl orthosilicate (TEOS) or tetramethyl orthosilicate (TMOS) in the presence of water and alcohol solvents, usually under basic conditions. In 1968, Stöber et al. reported the synthesis of spherical monodisperse silica nanoparticles using TEOS as the silicon alkoxide and an aqueous ethanol solution of ammonia and water (Stöber et al., 1968).

Fig. 5(c) is an illustration of particle synthesis mechanism. Silica particles are made into nanoparticles through a two-step reaction: hydrolysis and condensation (Ghimire and Jaroniec, 2021). In hydrolysis the –OR around the silicon in alkoxysilane is changed to –OH, with an alcohol in

the form of ROH as a byproduct. The alcohol byproduct is determined by the alkyl group of alkoxysilane. After the hydration reaction with Si(OH)₄, condensation proceeds as water escapes (Selvarajan et al., 2020). The size and distribution of the particles are affected by the reaction kinetics of the hydrolysis and condensation reactions, which are strongly influenced by the type of alkyl group of the alcohol and silicon alkoxide, the amount of base catalyst, and the temperature (Costa et al., 2003; Fernandes et al., 2019; Green et al., 2003; Plumeré et al., 2012). The technique allowed for the production of nanoparticles between 50 nm and 1 μm in diameter with a narrow distribution of spherical shapes (Fig. 5(d)). Silica synthesized with the Stöber method has inspired many research areas, including CMP slurries.

When synthesizing Stöber silica, the choice of alkoxysilane precursor (e.g., TEOS or TMOS) can affect the reactivity and overall properties of the synthesized nanoparticles. The alkyl in alkoxysilane acts as a leaving group during hydrolysis. The larger the molecular weight of the alkyl group serving as the leaving group, the slower the reaction rate (Costa et al., 2003). The hydrolysis reaction therefore proceeds in the order of methyl > ethyl > propyl. A slower hydrolysis reaction results in smaller particle size with a narrow size distribution, which helps create monodispersed particles. However, particles with slow reaction rate may lengthen the synthesis time and reduce reaction yields. In contrast, TMOS, which has higher reaction rate, leads to larger particles with a broader distribution. Due to its balanced properties, TEOS is the most commonly used alkoxysilane for silica synthesis.

The high cost of TEOS has been a persistent issue with Stöber silica. Soh et al. (1999) developed a process for synthesizing TMOS at a significantly lower unit cost by reacting silicon and methanol under copper catalyst. As a result, research on synthesizing monodisperse silica with reduced manufacturing costs has been reported. One method involves controlling the molar ratio of water to TMOS (Anderson and Carroll, 2011). A higher water-to-TMOS ratio accelerates hydrolysis and condensation reactions, producing smaller particles with a narrow size distribution. Temperature also plays a role in particle size and distribution. Higher temperatures accelerate hydrolysis and condensation, leading to smaller particles with a narrow size distribution. Conversely, lower temperatures decelerate reactions, resulting in larger particles with a broader size distribution.

The type and concentration of catalyst (acidic or basic) used in the Stöber process can significantly affect hydrolysis and condensation reaction rates and, therefore the size and morphology of silica nanoparticles. Acidic catalysts (e.g., HCl) tend to produce smaller particles, while basic catalysts (e.g., ammonia) often result in larger particles (Ghimire and Jaroniec, 2021). Adjusting the catalyst

concentration allows control of reaction kinetics and tuning of particle size.

In summary, the chemical composition variables of the Stöber method, such as alkoxysilane precursor, catalyst, solvent, water-to-precursor ratio, temperature, and reaction time, can significantly affect the synthesis results. By controlling these variables, researchers can tailor the size, shape, and properties of silica nanoparticles for various applications.

Stöber silica is synthesized in liquid phase reaction, has Newtonian behavior in its hydrophilic and rheological behavior due to the multiple silanol groups on its surface, and is highly dispersible. The IEP of silica synthesized using the sol–gel method can be affected by the washing process. Washing is used to remove residual reactants and impurities such as unreacted precursors, alcohols, and counterions (Ibrahim et al., 2010). The IEP of silica is closely related to the presence of silanol groups on the surface and the adsorption of counterions (De Keizer et al., 1998; Srinivasan et al., 1994; Szekeres et al., 2002; Wells et al., 2000). During the cleaning process, these counterions can be removed, changing the surface charge of silica particles and consequently the IEP. For example, if an ammonia catalyst remains on a silica particle, the IEP will shift to pH 4. This is because the positively charged ammonium ions remain inside the silica, making the surface charge positive.

Fig. 6 shows the results of CMP of SiO₂ film as a function of pH using silica dispersion according to particle synthesis method. In the case of fumed silica slurry, the removal rate occurs at strong base conditions above pH 10, and the removal rate decreases as it approaches pH 3. This is because fumed silica with low dispersion stability is prone to agglomeration if sufficient electrostatic attraction is not maintained, and active particles are reduced due to small contact area. Compared with Stöber silica, fumed silica is harder from a mechanical point of view due to fewer pores and a higher surface area, and therefore has a higher removal rate compared with Stöber silica when it is highly dispersible (Estel et al., 2010). In the case of Stöber

silica, the removal rate is also higher in acidic region, resulting from the higher dispersion stability of Stöber silica compared to fumed silica. However, at high pH, the contact area decreases because the zeta potential of the film is as high as that of Stöber silica.

4. Modification of silica nanoparticles

Stöber silica is also utilized in metal CMP of tungsten and copper films, in addition to SiO₂ films, due to its high acidity and ability to reduce scratches and defects. The slurry in which Stöber silica is dispersed contains chemical additives such as passivation agents, dispersants, inhibitors, and removal-rate enhancers to improve the zeta potential of silica in acidic conditions or increase selectivity and removal rates (Lee et al., 2016). However, predicting and controlling reactions in a slurry system can be challenging, as these additives act simultaneously on the film and abrasive silica nanoparticles. Consequently, ongoing research aims to improve CMP performance by modifying existing silica particles and enhancing their surface properties.

As illustrated in Fig. 7, several strategies to improve CMP performance are available for modifying silica. One is to reduce scratches and roughness by coating the surface of silica on a relatively soft core, creating a core–shell structure (Fig. 7(a)) (Chen et al., 2015b). Another is to enhance the removal rate by coating a harder shell on the silica core (Fig. 7(b)) (Ma et al., 2018). Some particles exhibit improved reactivity by embedding particles with a chemically catalytic effect on the silica surface (Fig. 7(c)) (Sun et al., 2022). Other particles have a controlled zeta potential or improved chemical reactivity through the doping of other metals (Fig. 7(d)) (Bykov et al., 2021). Finally, the zeta potential of particles can be controlled by substituting surface functional groups or reducing friction force by adjusting the hydrophilicity or hydrophobicity (Fig. 7(e)) (Björkegren et al., 2017). These strategies are designed to optimize the properties of silica particles for CMP applications, leading to superior performance in semiconductor manufacturing.

4.1 Core–shell structure: silica shell

Films made of copper or SiO₂, which are relatively soft, are susceptible to mechanical damage (Paik and Park, 2009). The use of hard and large particles during polishing can increase defect density, surface roughness, and scratches (Guo et al., 2013). To address this issue, composite materials made of polymers and silica are being explored as an alternative to traditional silica nanoparticles. These composites have relatively low hardness, which makes them less likely to cause mechanical damage during polishing. To reduce defects while maintaining removal rates, researchers have been investigating using organic/inorganic core–shell composites (polymers as the core material, with a silica coating on the surface) (Debnath and

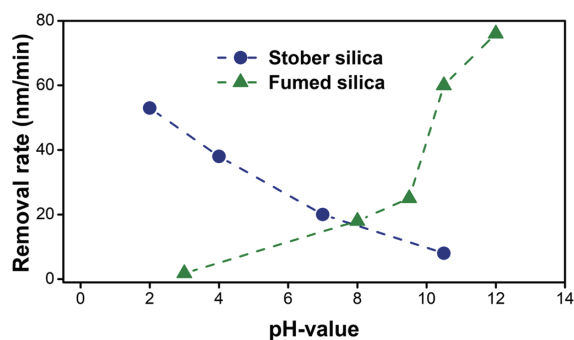


Fig. 6 SiO₂ film removal rate as a function of pH in an abrasive-based slurry according to a silica synthesis method. Reprinted with permission from Ref. (Estel et al., 2010). Copyright: (2010) Springer Nature.

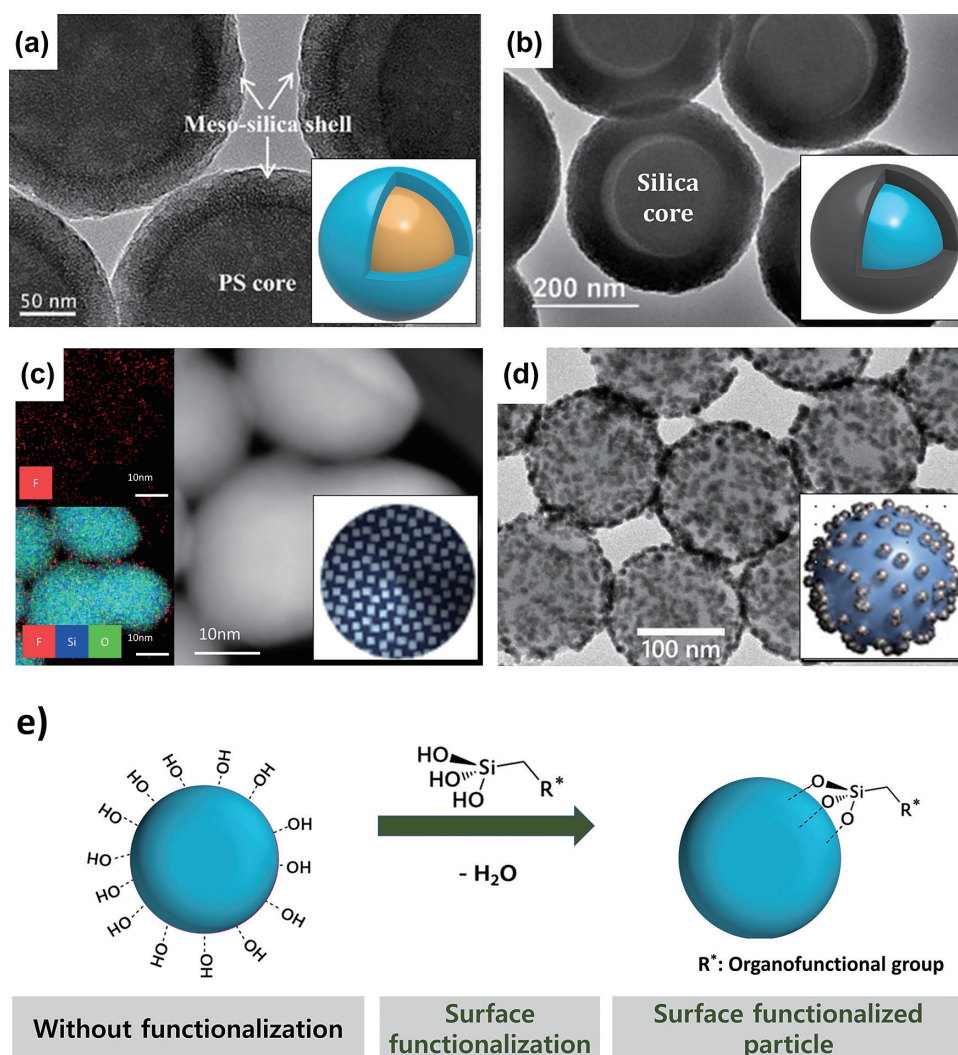


Fig. 7 Classifying silica abrasive surface modifications to improve CMP properties. **(a)** Core-shell structure of silica shell. Reprinted with permission from Ref. (Chen et al., 2015b). Copyright: (2015) Springer Nature. **(b)** Core-shell structure of silica core. Reprinted with permission from Ref. (Ma et al., 2018). Copyright: (2018) Elsevier. **(c)** Silica doped with other elements. Reprinted permission from Ref. (Sun et al., 2022). Copyright: (2022) Elsevier. **(d)** Silica dot-coated with other materials. Reprinted with permission from Ref. (Bykov et al., 2021) under the terms of the CC-BY 4.0 license. Copyright: (2021) The Authors, published by De Gruyter. **(e)** Surface functional group substituted silica. Reprinted with permission from Ref. (Björkegren et al., 2017). Copyright: (2017) Elsevier.

Khatua, 2011). This approach has shown promise in reducing defects while maintaining the desired level of material removal. Overall, the development of new composite materials for CMP films can improve the efficiency and quality of polishing processes while reducing the risk of damage to the finished materials.

When organic–inorganic composites are used as abrasives in CMP, polystyrene (PS) and PMMA are mainly used as core materials. PS and PMMA offer controllable properties, as they can produce particles of various sizes and shapes depending on the conditions required in CMP (Lee, 2000). Using PS and PMMA is relatively inexpensive, and both are widely available polymeric materials, helping reduce process costs. PS and PMMA are chemically and thermally stable, making them suitable for most process environments, and this stability contributes to high yields and quality in CMP processes. When organic materi-

als such as PS and PMMA are combined with inorganic materials, the interaction between abrasive particles increases, and the flexibility of the organic material improves, resulting in enhanced abrasive effects (Chen et al., 2016).

Chen et al., (2014) experimented with measuring modulus of PS/silica core–shell nanocomposites using AFM. They functionalized the surface of a 450 nm PS particle with azodiisobutyramidine dihydrochloride and allowed it to react with TEOS to coat a 10 nm SiO₂ shell. As a result, the Young's modulus of the PS particle, originally 2.85 GPa, increased by a factor of approximately 1.8, to 5.1 GPa, when it became a composite. Considering that the Young's modulus of bulk SiO₂ is approximately 70 GPa, the PS/silica composite is clearly a relatively soft abrasive. Zhang et al. (2019) reported that the value of the Young's modulus increased as the thickness of the SiO₂ shell increased. When performing CMP on SiO₂ films with core–shell

particles, the root mean squared value decreased from 0.48 nm to 0.37 nm compared with silica particles of the same size. This reduction can be attributed to the lower Young's modulus of the nanoparticles compared to that of the silica particles, resulting in a decreased volume indented during CMP and improved contact area.

Chen et al. (2017) compared solid silica and mesoporous silica coatings on PS surfaces. When coating approximately 200 nm PS particles with 30 nm silica shell, the mesoporous silica shell exhibited similar roughness of 0.22 nm and 0.25 nm, respectively, compared with the solid silica shell. The removal rate was 123 nm/min for mesoporous silica shell and 47 nm/min for solid silica shell, which can be explained by the higher contact area offered with mesoporous silica compared to solid silica.

4.2 Core-shell structure: silica core

Compared with silica, using silica nanoparticles in CMP for materials with high hardness can be challenging, as an adequate removal rate may be difficult to achieve. However, harder particles also tend to have reduced dispersion stability and can be damaged by scratches (Lei and Zhang, 2007). As a result, researchers have been attempting to create particles with both good dispersion stability and acceptable removal rate by coating a silica core with other materials with greater hardness (Dai et al., 2020; Lei and Zhang, 2007). This approach combine the advantages of both components, resulting in an improved abrasive for CMP applications involving harder materials. Table 4 summarizes the CMP results for composite particles with different core-shell structures using silica as core material.

Dai et al. (2020) coated SiC on a silica surface and applied a core-shell composite for CMP of a sapphire film with a high Mohs hardness of 9.0. SiC has Mohs hardness of 9 to 9.5, which enhances the mechanical properties of silica. Moreover, silica's high zeta potential under basic conditions gives it superior dispersion stability compared with SiC particles. In their experiments, SiC had a zeta potential of -44.6 mV at pH 10, while the silica-SiC composite had a zeta potential of -68.8 mV. Consequently, the removal rate was approximately double that of silica and 1.8 times that of SiC, and the respective roughness values were 1.9 nm and 1.97 nm for silica and SiC. The core-shell composite achieved a roughness of 1.52 nm.

Lei and Zhang (2007) coated alumina on silica surface to increase the polishing rate and flatness of nickel phosphorus (NiP). Alumina particles had a zeta potential of -40.8 mV, whereas silica-alumina composite achieved greater dispersion stability at -60.1 mV. In this experiment, while the polishing rate was lower for the core-shell composite compared with alumina, the roughness decreased by approximately 33 %.

Ding et al. (2022) employed a silica-diamond composite for ZrO₂ CMP. In this case, a core-shell composite using

silica as the core had a higher zeta potential compared with a nanodiamond, ranging from -35 mV to -55 mV, leading to improvements in both removal rate and roughness, as confirmed by CMP results.

Although the same silica material was used in other core-shell composites, one study compared solid silica and core-shell particles coated with mesoporous silica on solid silica (Chen et al., 2018). Mesoporous silica has larger contact area than solid silica but mechanically weaker. To enhance the mechanical strength and increase the contact area, core-shell structure was adopted, which resulted in an improved removal rate.

4.3 Metal doped silica nanoparticles

Increasing the absolute value of zeta potential of silica can further enhance its dispersion stability. Metal-doped silica modification can maintain the spherical shape of silica while shifting its IEP. Silica is a material in which Si⁴⁺ ions form covalent bonds with oxygen (Tao et al., 2010). Doping or substituting the Si⁴⁺ site with metal ions carrying a 3+ charge increases the negative zeta potential of silica and shifts the IEP toward the acidic range, or even gives it a negative charge throughout the entire pH range. This allows for high dispersion stability in the challenging pH 2–3 range of silica's IEP, making it suitable for use in CMP slurries. The conditions for metals used in silica doping require the metal ions to be similar in size to silicon ions and carry a charge lower than 4+.

Doping with Sm³⁺, Nb³⁺, Al³⁺, Fe³⁺, and Co³⁺ ions, which meet these criteria has been reported (Lei et al., 2019; Liu and Lei, 2017; Ma et al., 2015; Sun et al., 2022). Silica doped with these ions maintains smooth surface and has higher zeta potential than un-doped silica, resulting in higher dispersion stability. While it is theoretically possible to dope with ions carrying a charge higher than Si⁴⁺ to achieve positive charge, there are no reports of this being accomplished. The size of ions carrying 5+ charge is presumably not suitable for silica doping.

In a report on silica doped with Fe³⁺ ions, Sun et al. (2022) clarified the conditions and mechanism for synthesizing doped silica. Silica dissolves as tetrahedral Si(OH)₄ in highly alkaline conditions at high temperatures (Niibori et al., 2000). At the same time, metal hydroxides with similar tetrahedral structure can replace vacant Si(OH)₄ sites. According to Sun et al. (2022), the synthesis of pH is crucial in this reaction and proceeds under conditions in which Si(OH)₄ can dissolve. Fig. 8 illustrates Fe³⁺ ion doping and coating as a function of pH. At pH 11, the silica surface dissolves as Si(OH)₄, and Fe³⁺ exists as Fe(OH)₄⁻, allowing the doping reaction to proceed. In contrast, at pH 5, Si(OH)₄ dissolution rarely occurred, and iron hydroxide coated the silica surface.

Using such reactions, researchers synthesized silica particles with various metal-ion doping and high dispersion

Table 4 CMP results using core-shell composite abrasive.

Core	Shell	pH	CMP equipment	CMP pad	Substrate	Removal rate	Roughness	Reference
Silica	—	10	UNIPOL-1502 (Kejing Co. Ltd.)	Polyurethane pad (DOW Chemical)	Sapphire	0.15 $\mu\text{m}/\text{h}$	Ra: 1.90 nm	(Dai et al., 2020)
SiC	—	10.5	UNIPOL-1502 (Kejing Co. Ltd.)	Polyurethane pad (DOW Chemical)	Sapphire	0.17 $\mu\text{m}/\text{h}$	Ra: 1.97 nm	(Dai et al., 2020)
SiC	Silica	10.5	UNIPOL-1502 (Kejing Co. Ltd.)	Polyurethane pad (DOW Chemical)	Sapphire	0.31 $\mu\text{m}/\text{h}$	Ra: 1.52 nm	(Dai et al., 2020)
Alumina	—	9–10	SPEED-FAM-16B-4M (SPEEDFAM Co. Ltd.)	Rodel porous polyurethane pad (DOW Chemical)	NiP	540 nm/min	Ra: 0.7 nm	(Lei and Zhang, 2007)
Alumina	Silica	9–10	SPEED-FAM-16B-4M (SPEEDFAM Co. Ltd.)	Rodel porous polyurethane pad (DOW Chemical)	NiP	440 nm/min	Ra: 0.45 nm	(Lei and Zhang, 2007)
Silica	—	10	UNIPOL-1000S (Kejing Co. Ltd.)	Rodel porous polyurethane pad (DOW Chemical)	ZrO ₂	0.142 $\mu\text{m}/\text{h}$	Ra: 2.49 nm	(Ding et al., 2022)
Nano diamond	—	10	UNIPOL-1000S (Kejing Co. Ltd.)	Rodel porous polyurethane pad (DOW Chemical)	ZrO ₂	0.91 $\mu\text{m}/\text{h}$	Ra: 9.92 nm	(Ding et al., 2022)
Nano diamond	Silica	10	UNIPOL-1000S (Kejing Co. Ltd.)	Rodel porous polyurethane pad (DOW Chemical)	ZrO ₂	1.062 $\mu\text{m}/\text{h}$	Ra: 2.26 nm	(Ding et al., 2022)
Silica (solid)	—	8	TegraForce-1/TrgraPol-15 (Struers)	Porous polyurethane pad (MD-Chem)	SiO ₂	137 $\mu\text{m}/\text{min}$	RMS: 0.343 nm	(Chen et al., 2018)
Silica (solid)	Mesoporous silica	8	TegraForce-1/TrgraPol-15 (Struers)	Porous polyurethane pad (MD-Chem)	SiO ₂	269 nm/min	RMS: 0.203 nm	(Chen et al., 2018)

stability. These particles were applied in CMP to achieve higher removal rates and planarity. This method modifies silica properties without significantly altering its mechanical properties.

4.4 Metal compound dot-coated silica nanoparticles

Silica nanoparticles are chemically unreactive, and it is unrealistic to expect a catalytic effect from silica alone in CMP (Eppler et al., 2000). However, silica can serve as template for highly reactive catalysts. In other words, by coating the surface of silica particles with highly reactive catalysts, it is possible to synthesize abrasives with catalytic effects and apply them to CMP (Giraldo et al., 2007; Janaun and Ellis, 2011).

Zhang et al. (2017) investigated the use of an Ag₂O–silica composite to enhance the removal rate of sapphire CMP. Ag⁺ in Ag₂O acts as a catalyst to react Al₂O₃ with SiO₂, forming aluminum silicon oxide (Al_xSi_yO). The relatively weak Al_xSi_yO on the sapphire surface can be easily

removed by silica abrasive, ensuring a high removal rate in the hard sapphire CMP. Yin et al. applied MgO-doped silica as a more affordable alternative to expensive Ag₂O to improve the removal rate of sapphire CMP. Adding MgO under alkaline conditions causes the Al–O–Al chemical bonds to break more easily, and the formed softening layer is more easily removed from the surface. At the same time, reactions of MgO with the sapphire substrate surface produced MgAl₂O₄. The reaction products of H₂O, MgO, SiO₂, and Al₂O₃, such as Al₂Si₂O₇–2H₂O, MgAl₂O₄, and the softening layer of Al₂SiO₅, can be easily removed by mechanical action.

Kang et al. (2010) studied silica-containing iron metal for CMP of tungsten. In this process, H₂O₂ was added to form WO₃ on the tungsten surface. The metal catalyst decomposed H₂O₂ through Fenton reaction, generating highly reactive OH radicals. The iron metal on silica surface acted as a catalyst for decomposing H₂O₂. Kang et al. reported achieving the same level of CMP performance by comparing two cases: one in which iron ion was added as an

additive, and another where iron metal–silica composite was applied. To address the issue of poor dispersion stability of silica in the acidic region of pH 2, where iron metal–silica is typically applied, Kim et al. (2017) proposed a CuO–silica composite that can be utilized at pH 6. CuO can decompose H_2O_2 through Fenton-like reaction, which also occurs in neutral regions. They reported the successful use of silica particles with CuO catalyst.

4.5 Functionalization of surfaces on silica nanoparticles

Surface functionalization of silica nanoparticles involves

altering the particle surface properties of silica by attaching specific functional groups or molecules. This process is crucial in enhancing the attributes of silica nanoparticles for a range of applications, such as drug delivery, sensors, catalysis, and environmental remediation (Nayl et al., 2022). CMP is often employed to enhance surface charge, control adsorption to passivation agents or films, and manage friction (Seo, 2021).

Silane coupling agents such as organosilanes are commonly used to functionalize silica nanoparticle surfaces (Karnati et al., 2020). These molecules possess a reactive silicon-containing group (e.g., alkoxy silane or chlorosilane)

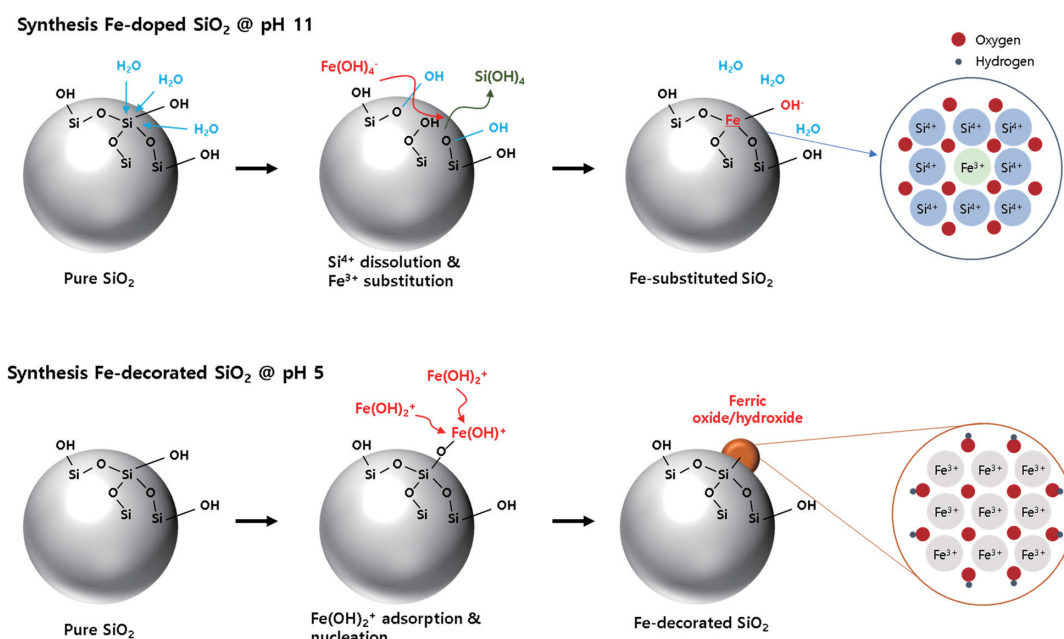


Fig. 8 Schematic from mechanistic perspective of pH-dependent doping and coating of Fe on silica surfaces. Reprinted with permission from Ref. (Sun et al., 2022). Copyright: (2022) Elsevier B.V.

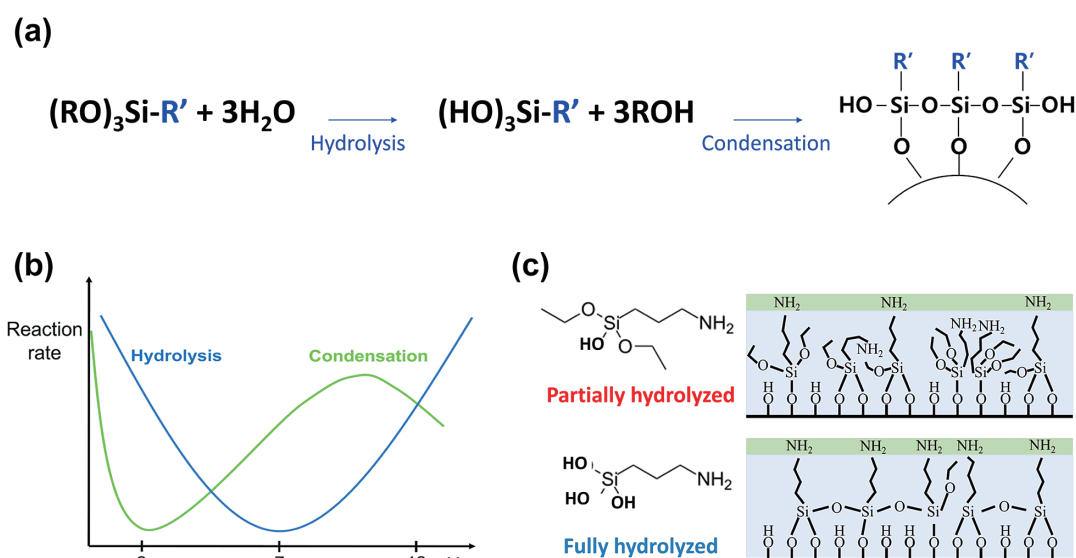
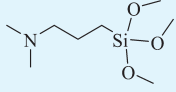
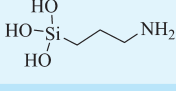
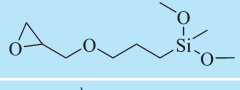
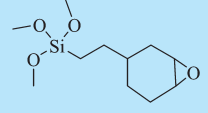
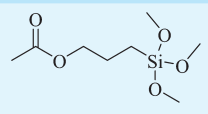
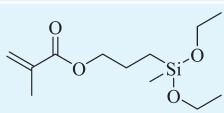
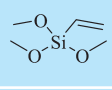
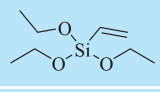
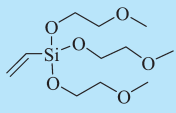
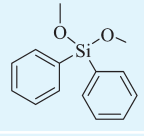
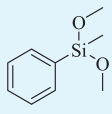
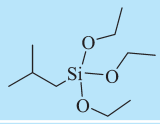
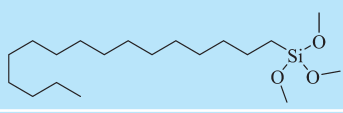

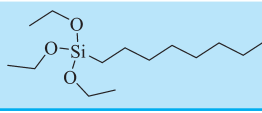


Fig. 9 (a) Reaction mechanism for the surface modification of silica nanoparticles using silane coupling agent. (b) Effect of pH on hydrolysis and condensation rates. Reprinted with permission from Ref. (Gutiérrez-Climente et al., 2021). Copyright: (2021) The Royal Society of Chemistry. (c) The structure of silica surface functional groups upon partially or fully hydrolyzed organosilane (APTES).

Table 5 Organosilane coupling agents for improving properties of silica nanoparticles.

Classification	Chemical name	Molecular structure	Properties	Reference
Amino silanes	(N,N-Dimethyl-3-aminopropyl)trimethoxysilane		Increased interaction with surfactants	(Wang et al., 2019)
	3-aminopropylsilane		IEP shift (Increasing positive charge)	(Wang et al., 2019)
Epoxy silanes	3-Glycidoxypromethylmethyldimethoxysilane		Improving adhesion to film	(Pan et al., 2016)
	2-(3,4-Epoxyhexahydro-2H-pyran-2-yl)ethyltrimethoxysilane		Improving adhesion to film	(Pan et al., 2016)
Acryl silanes	3-Acetoxypropyltrimethoxysilane		Supplying electrophilic reaction sites	(Göppert et al., 2023)
	3-Methacryloxypropylmethyldiethoxysilane			(Göppert et al., 2023)
Vinyl silanes	Vinyltrimethoxysilane		Supplying nucleophilic reaction sites	(Nasab and Kiasat, 2016)
	Triethoxyvinylsilane			(Nasab and Kiasat, 2016)
	Vinyl tris(2-methoxyethoxy) silane			(Nasab and Kiasat, 2016)
Phenyl silanes	Diphenyldimethoxysilane		Increased interaction with surfactants	(Chen et al., 2004)
	Phenylmethyldimethoxysilane			(Chen et al., 2004)
Alkyl silanes	Isobutyltriethoxysilane		Improving hydrophobic properties Decreasing friction force	(Wang and Zhang, 2020)
	n-Hexadecyltrimethoxysilane			(Wang and Zhang, 2020)
	Dodecyltrimethoxysilane			(Wang and Zhang, 2020)
	Triethoxyoctylsilane			(Wang and Zhang, 2020)

that can bind to the silanol groups present on the silica surface, and an organic functional group (e.g., an amine, thiol, or carboxyl) capable of reacting with other molecules or biomolecules (Franz and Wilson, 2013). By selecting appropriate silane-coupling agent, various functional groups can be introduced onto the silica surface. Fig. 9(a) depicts the reaction between organosilane and silanol groups on the surface of silica nanoparticle. Initially, the organosilane reacts with water and undergoes hydrolysis to form hydroxyl groups, and then the functional groups of the organosilane are exposed on the silica surface as the hydroxyl groups condense on the silanol groups on the silica surface (Li et al., 2021).

For successful functionalization, it is crucial to ensure that no particles form due to condensation between organosilanes. Fig. 9(b) depicts the rate of hydrolysis and condensation reactions depending on pH (Gutiérrez-Climente et al., 2021; Chiriac et al., 2010). In highly acidic or basic conditions, in which both reaction rates are high, organosilanes react primarily with each other, leading to particle formation (Argekar et al., 2013). However, at a neutral pH of 7, the reaction rate is too slow, resulting in partial hydrolysis (Fig. 9(c)), with bridging between methoxy groups. The functionalization reaction is therefore typically carried out in a slightly acidic environment of pH 4–6. Table 5 categorizes organosilanes and summarizes the properties of silica during functionalization. For complete hydrolysis through functionalization reaction of each organosilane, it is essential to control the concentration of organosilanes and temperature, taking into account the number of silanol groups on the silica nanoparticles.

5. Conclusion

Silica nanoparticles are used extensively in CMP, and their performance can be improved through modification techniques such as surface functionalization, core-shell structure formation, coating or doping with other metal atoms. These particles reduce defects and scratches, improve flatness and uniformity, and increase the removal rate and selectivity. The careful selection and utilization of nanoparticles with these properties therefore has significant impact on the efficiency of CMP. This review offers valuable information on how to improve the quality of products and reduce costs in the semiconductor industry. The development of silica nanoparticles is currently an important area of research. Different synthesis methods were applied to CMP slurries and their properties were investigated. Further study of their properties and synthesis methods will be of great help in creating better products in semiconductor industry.

Acknowledgments

G. Lee, K. Lee and S. Sun. contributed equally to this work. T. Song and U. Paik reviewed and revised the manu-

script. This work was supported by the Energy Technology Human Resource Development Project(202300000000101) of the Ministry of Trade, Industry and Energy (KITIE) and the Samsung Electronics University R&D Program (202200000630003). All authors have given approval to the final version of the manuscript.

Conflict of Interest

The authors declare no conflicts of interest.

References

- Ahn Y., Yoon J.-Y., Baek C.-W., Kim Y.-K., Chemical mechanical polishing by colloidal silica-based slurry for micro-scratch reduction, *Wear*, 257 (2004) 785–789.
<https://doi.org/10.1016/j.wear.2004.03.020>
- Anderson A.M., Carroll M.K., Hydrophobic silica aerogels: review of synthesis, properties and applications, *Aerogels Handbook*, (2011) 47–77. https://doi.org/10.1007/978-1-4419-7589-8_3
- Argekar S.U., Kirley T.L., Schaefer D.W., Determination of structure-property relationships for 3-aminopropyltriethoxysilane films using X-ray reflectivity, *Journal of Materials Research*, 28 (2013) 1118–1128. <https://doi.org/10.1557/jmr.2013.54>
- Armini S., De Messemacker J., Whelan C., Moinpour M., Maex K., Composite polymer core-ceria shell abrasive particles during oxide CMP: a defectivity study, *Journal of the Electrochemical Society*, 155 (2008) H653. <https://doi.org/10.1149/1.2949085>
- Babchin A.J., Schramm L.L., Osmotic repulsion force due to adsorbed surfactants, *Colloids and Surfaces B: Biointerfaces*, 91 (2012) 137–143. <https://doi.org/10.1016/j.colsurfb.2011.10.050>
- Barthel H., Rösch L., Weis J., Chapter 91, Fumed silica-production, properties, and applications, in: Auner N. and Weis J. (Eds.), *Organosilicon Chemistry Set: From Molecules to Materials*, ISBN: 9783527292547, 2005, pp. 761–778.
<https://doi.org/10.1002/9783527619894.ch91>
- Basim G., Adler J., Mahajan U., Singh R., Moudgil B., Effect of particle size of chemical mechanical polishing slurries for enhanced polishing with minimal defects, *Journal of the Electrochemical Society*, 147 (2000) 3523. <https://doi.org/10.1149/1.1393931>
- Bebie J., Schoonen M.A., Fuhrmann M., Strongin D.R., Surface charge development on transition metal sulfides: an electrokinetic study, *Geochimica et Cosmochimica Acta*, 62 (1998) 633–642.
[https://doi.org/10.1016/S0016-7037\(98\)00058-1](https://doi.org/10.1016/S0016-7037(98)00058-1)
- Bergström L., Hamaker constants of inorganic materials, *Advances in Colloid and Interface Science*, 70 (1997) 125–169.
[https://doi.org/10.1016/S0001-8686\(97\)00003-1](https://doi.org/10.1016/S0001-8686(97)00003-1)
- Beyer K., The dynamics of the CMP discovery for device applications in IBM, 2015 International Conference on Planarization/CMP Technology (ICPT), IEEE, (2015).
https://doi.org/10.1147/OUBUTSU.90.2_119
- Björkegren S., Nordstierna L., Törnroona A., Palmqvist A., Hydrophilic and hydrophobic modifications of colloidal silica particles for Pickering emulsions, *Journal of Colloid and Interface Science*, 487 (2017) 250–257. <https://doi.org/10.1016/j.jcis.2016.10.031>
- Bykov A.Y., Roth D.J., Sartorello G., Salmón-Gamboa J.U., Zayats A.V., Dynamics of hot carriers in plasmonic heterostructures, *Nanophotonics*, 10(2021)2929–2938. <https://doi.org/10.1515/nanoph-2021-0278>
- Chen A., Chen Y., Zhao X., Wang Y., Core/shell structured PS/mSiO₂ hybrid particles: controlled preparation, mechanical property, and their size-dependent CMP performance, *Journal of Alloys and Compounds*, 779 (2019) 511–520.
<https://doi.org/10.1016/j.jallcom.2018.11.314>
- Chen A., Mu W., Chen Y., Compressive elastic moduli and polishing performance of non-rigid core/shell structured PS/SiO₂ composite abrasives evaluated by AFM, *Applied Surface Science*, 290 (2014) 433–439. <https://doi.org/10.1016/j.apsusc.2013.11.100>
- Chen X., Huang Q., Hao W., Ding C., Wang Y., Zeng H., Controlling of fumed silica particle size uniform production process based on

- burner fluid dynamic simulation, *Industrial & Engineering Chemistry Research*, 61 (2022) 7235–7244.
<https://doi.org/10.1021/acs.iecr.2c00606>
- Chen Y.-C., Lin H.-C., Lee Y.-D., The effects of phenyltrimethoxysilane coupling agents on the properties of PTFE/silica composites, *Journal of Polymer Research*, 11 (2004) 1–7.
<https://doi.org/10.1023/B:JPOL.0000021757.94577.a3>
- Chen Y., Chen A., Qin J., Polystyrene core–silica shell composite particles: effect of mesoporous shell structures on oxide CMP and mechanical stability, *RSC Advances*, 7 (2017) 6548–6558.
<https://doi.org/10.1039/c6ra26437a>
- Chen Y., Li Z., Qian C., Core–shell structured polystyrene coated silica composite abrasives with homogeneous shells: the effects of polishing pressure and particle size on oxide-CMP, *Precision Engineering*, 43 (2016) 71–77. <https://doi.org/10.1016/j.precisioneng.2015.06.011>
- Chen Y., Qian C., Miao N., Atomic force microscopy indentation to determine mechanical property for polystyrene–silica core–shell hybrid particles with controlled shell thickness, *Thin Solid Films*, 579 (2015a) 57–63. <https://doi.org/10.1016/j.tsf.2015.02.049>
- Chen Y., Qin J., Wang Y., Li Z., Core/shell composites with polystyrene cores and meso-silica shells as abrasives for improved chemical mechanical polishing behavior, *Journal of Nanoparticle Research*, 17 (2015b) 1–11. <https://doi.org/10.1007/s11051-015-3172-5>
- Chen Y., Zuo C., Chen A., Core/shell structured $\text{SiO}_2/\text{mSiO}_2$ composite particles: the effect of the core size on oxide chemical mechanical polishing, *Advanced Powder Technology*, 29 (2018) 18–26.
<https://doi.org/10.1016/j.apt.2017.09.020>
- Chiriac A.P., Neamtu I., Nita L.E., Nistor M.T., Sol gel method performed for biomedical products implementation, *Mini Reviews in Medicinal Chemistry*, 10 (2010) 990–1013.
<https://doi.org/10.2174/1389557511009010990>
- Choi W., Mahajan U., Lee S.-M., Abiad J., Singh R.K., Effect of slurry ionic salts at dielectric silica CMP, *Journal of the Electrochemical Society*, 151 (2004) G185. <https://doi.org/10.1149/1.1644609>
- Costa C.A., Leite C.A., Galembeck F., Size dependence of Stöber silica nanoparticle microchemistry, *The Journal of Physical Chemistry B*, 107 (2003) 4747–4755. <https://doi.org/10.1021/jp027525t>
- Croissant J.G., Butler K.S., Zink J.I., Brinker C.J., Synthetic amorphous silica nanoparticles: toxicity, biomedical and environmental implications, *Nature Reviews Materials*, 5 (2020) 886–909.
<https://doi.org/10.1038/s41578-020-0230-0>
- Dai S., Lei H., Fu J., Preparation of SiC/SiO_2 hard core–soft shell abrasive and its CMP behavior on sapphire substrate, *Journal of Electronic Materials*, 49 (2020) 1301–1307.
<https://doi.org/10.1007/s11664-019-07683-9>
- De Keizer A., Van der Ent E., Koopal L., Surface and volume charge densities of monodisperse porous silicas, *Colloids and Surfaces A: Physicochemical and Engineering Aspects*, 142 (1998) 303–313.
[https://doi.org/10.1016/s0927-7757\(98\)00268-4](https://doi.org/10.1016/s0927-7757(98)00268-4)
- Debnath D., Khatua B., Preparation by suspension polymerization and characterization of polystyrene (PS)-poly (methyl methacrylate) (PMMA) core-shell nanocomposites, *Macromolecular Research*, 19 (2011) 519–527. <https://doi.org/10.1007/s13233-011-0607-4>
- Ding R., Lei H., Chen C., Zhang Z., Preparation of the nanodiamond@ SiO_2 abrasive and its effect on the polishing performance of zirconia ceramics, *ECS Journal of Solid State Science and Technology*, 11 (2022) 064002. <https://doi.org/10.1149/2162-8777/ac757e>
- Dorobantu L.S., Bhattacharjee S., Foght J.M., Gray M.R., Analysis of force interactions between AFM tips and hydrophobic bacteria using DLVO theory, *Langmuir*, 25 (2009) 6968–6976.
<https://doi.org/10.1021/la9001237>
- Ein-Eli Y., Starosvetsky D., Review on copper chemical–mechanical polishing (CMP) and post-CMP cleaning in ultra large system integrated (ULSI)—An electrochemical perspective, *Electrochimica Acta*, 52 (2007) 1825–1838. <https://doi.org/10.1016/j.electacta.2006.07.039>
- Eppler A.S., Rupprechter G., Anderson E.A., Somorjai G.A., Thermal and chemical stability and adhesion strength of Pt nanoparticle arrays supported on silica studied by transmission electron microscopy and atomic force microscopy, *The Journal of Physical Chemistry B*, 104 (2000) 7286–7292. <https://doi.org/10.1021/jp0006429>
- Estel K., Künzelmann U., Bartha J.W., Meyer E.P., Barthel H., Influence of ionic strength and pH-value on the silicon dioxide polishing behaviour of slurries based on pure silica suspensions, *MRS Online Proceedings Library*, 1249 (2010) 402.
<https://doi.org/10.1557/proc-1249-e04-02>
- Feng X., Sayle D.C., Wang Z.L., Paras M.S., Santora B., Sutorik A.C., Sayle T.X., Yang Y., Ding Y., Wang X., Converting ceria polyhedral nanoparticles into single-crystal nanospheres, *Science*, 312 (2006) 1504–1508. <https://doi.org/10.1002/chin.200636200>
- Fernandes R.S., Raimundo Jr I.M., Pimentel M.F., Revising the synthesis of Stöber silica nanoparticles: a multivariate assessment study on the effects of reaction parameters on the particle size, *Colloids and Surfaces A: Physicochemical and Engineering Aspects*, 577 (2019) 1–7.
<https://doi.org/10.1016/j.colsurfa.2019.05.053>
- Franz A.K., Wilson S.O., Organosilicon molecules with medicinal applications, *Journal of Medicinal Chemistry*, 56 (2013) 388–405.
<https://doi.org/10.1021/jm3010114>
- Fury M.A., The early days of CMP, *Solid State Technology*, 40 (1997) 81–84.
- Garrett P.R., Defoaming: Theory and Industrial Applications, 1st edition, CRC Press, 2017, ISBN: 9780367402617.
<https://doi.org/10.1201/9781315140827>
- Ghimire P.P., Jaroniec M., Renaissance of Stöber method for synthesis of colloidal particles: new developments and opportunities, *Journal of Colloid and Interface Science*, 584 (2021) 838–865.
<https://doi.org/10.1016/j.jcis.2020.10.014>
- Giraldo L.F., López B.L., Pérez L., Urrego S., Sierra L., Mesa M., Mesoporous silica applications, *Macromolecular Symposia*, 258 (2007) 129–141. <https://doi.org/10.1002/masy.200751215>
- Göppert A.-K., Gonzalez-Rubio G., Schnitzlein S., Cölfen H., A nanoparticle-based model system for the study of heterogeneous nucleation phenomena, *Langmuir*, 39 (2023) 3580–3588.
<https://doi.org/10.1021/acs.langmuir.2c03034>
- Green D., Lin J., Lam Y.-F., Hu M.-C., Schaefer D.W., Harris M., Size, volume fraction, and nucleation of Stober silica nanoparticles, *Journal of Colloid and Interface Science*, 266 (2003) 346–358.
[https://doi.org/10.1016/s0021-9797\(03\)00610-6](https://doi.org/10.1016/s0021-9797(03)00610-6)
- Guedes M., Ferreira J.M., Ferro A.C., A study on the aqueous dispersion mechanism of CuO powders using Tiron, *Journal of Colloid and Interface Science*, 330 (2009) 119–124.
<https://doi.org/10.1016/j.jcis.2008.10.057>
- Gun'ko V., Zarko V., Leboda R., Voronin E., Chibowski E., Pakhlov E., Influence of modification of fine silica by organosilicon compounds on particle-particle interaction in aqueous suspensions, *Colloids and Surfaces A: Physicochemical and Engineering Aspects*, 132 (1998) 241–249. [https://doi.org/10.1016/s0927-7757\(97\)00184-2](https://doi.org/10.1016/s0927-7757(97)00184-2)
- Guo D., Xie G., Luo J., Mechanical properties of nanoparticles: basics and applications, *Journal of Physics D: Applied Physics*, 47 (2013) 013001. <https://doi.org/10.1088/0022-3727/47/1/013001>
- Gutiérrez-Climente R., Clavié M., Dumy P., Mehdi A., Subra G., Sol–gel process: the inorganic approach in protein imprinting, *Journal of Materials Chemistry B*, 9 (2021) 2155–2178.
<https://doi.org/10.1039/d0tb02941f>
- Haba S., Fukuda K., Ohta Y., Koubuchi Y., Katouda T., Fumed silica slurry stabilizing methods for chemical mechanical polishing, *Japanese Journal of Applied Physics*, 42 (2003) 418.
<https://doi.org/10.1143/jjap.42.418>
- Hamaker H.C., The London—van der Waals attraction between spherical particles, *Physica*, 4 (1937) 1058–1072.
[https://doi.org/10.1016/S0031-8914\(37\)80203-7](https://doi.org/10.1016/S0031-8914(37)80203-7)
- Hayashi Y., Sakurai M., Nakajima T., Hayashi K., Sasaki S., Chikaki S.-i., Kunio T.K.T., Ammonium-salt-added silica slurry for the chemical mechanical polishing of the interlayer dielectric film planarization in ULSI's, *Japanese Journal of Applied Physics*, 34 (1995) 1037.
<https://doi.org/10.1143/jjap.34.1037>
- Hwang H.-S., Kang H.-G., Park J.-H., Paik U., Park H.-S., Park J.-G., Effect of alkaline agent with organic additive in colloidal silica slurry on polishing rate selectivity of polysilicon-to- SiO_2 in polysilicon CMP, *ECS Transactions*, 13 (2008) 67.
<https://doi.org/10.1149/ma2008-01/17/692>

- Hyde E.D., Seyfaee A., Neville F., Moreno-Atanasio R., Colloidal silica particle synthesis and future industrial manufacturing pathways: a review, *Industrial & Engineering Chemistry Research*, 55 (2016) 8891–8913. <https://doi.org/10.1021/acs.iecr.6b01839>
- Ibrahim I.A., Zikry A., Sharaf M.A., Preparation of spherical silica nanoparticles: Stober silica, *Journal of American Science*, 6 (2010) 985–989. <<https://picture.iczhiku.com/resource/paper/WYkdoklpfJzOtCvn.pdf>> accessed 08.11.2023.
- Ishida N., Craig V., Direct measurement of interaction forces between surfaces in liquids using atomic force microscopy, *KONA Powder and Particle Journal*, 36 (2019) 187–200. <https://doi.org/10.14356/kona.2019013>
- Janaun J., Ellis N., Role of silica template in the preparation of sulfonated mesoporous carbon catalysts, *Applied Catalysis A: General*, 394 (2011) 25–31. <https://doi.org/10.1016/j.apcata.2010.12.016>
- Jin Y., Song K., Gellermann N., Huang Y., Printing of hydrophobic materials in fumed silica nanoparticle suspension, *ACS Applied Materials & Interfaces*, 11 (2019) 29207–29217. <https://doi.org/10.1021/acsami.9b07433>
- Kang Y.-J., Prasad Y.N., Kim I.-K., Jung S.-J., Park J.-G., Synthesis of Fe metal precipitated colloidal silica and its application to W chemical mechanical polishing (CMP) slurry, *Journal of Colloid and Interface Science*, 349 (2010) 402–407. <https://doi.org/10.1016/j.jcis.2010.04.083>
- Kanungo S.B., Physicochemical properties of MnO₂ and MnO₂ CuO and their relationship with the catalytic activity for H₂O₂ decomposition and CO oxidation, *Journal of Catalysis*, 58 (1979) 419–435. [https://doi.org/10.1016/0021-9517\(79\)90280-x](https://doi.org/10.1016/0021-9517(79)90280-x)
- Kappl M., Butt H.J., The colloidal probe technique and its application to adhesion force measurements, *Particle & Particle Systems Characterization*, 19 (2002) 129–143. [https://doi.org/10.1002/1521-4117\(200207\)19:3<129::AID-PPSC129>3.0.CO;2-G](https://doi.org/10.1002/1521-4117(200207)19:3<129::AID-PPSC129>3.0.CO;2-G)
- Karnati S.R., Oldham D., Fini E.H., Zhang L., Application of surface-modified silica nanoparticles with dual silane coupling agents in bitumen for performance enhancement, *Construction and Building Materials*, 244 (2020) 118324. <https://doi.org/10.1016/j.conbuildmat.2020.118324>
- Kawaguchi M., Dispersion stability and rheological properties of silica suspensions in aqueous solutions, *Advances in Colloid and Interface Science*, 284 (2020) 102248. <https://doi.org/10.1016/j.cis.2020.102248>
- Khan S.A., Günther A., Schmidt M.A., Jensen K.F., Microfluidic synthesis of colloidal silica, *Langmuir*, 20 (2004) 8604–8611. <https://doi.org/10.1002/adma.200700127>
- Khavryutchenko V., Barthel H., Nikitina E., Fumed silica synthesis: from molecules, protoparticles and primary particles to aggregates and agglomerates, *Macromolecular Symposia*, 169 (2001) 7–18. [https://doi.org/10.1002/1521-3900\(200105\)169:1<7::AID-MASY7>3.0.CO;2-5](https://doi.org/10.1002/1521-3900(200105)169:1<7::AID-MASY7>3.0.CO;2-5)
- Kim E., Lee J., Park Y., Shin C., Yang J., Kim T., Shape classification of fumed silica abrasive and its effects on chemical mechanical polishing, *Powder Technology*, 381 (2021) 451–458. <https://doi.org/10.1016/j.powtec.2020.11.058>
- Kim K., Yi D.K., Paik U., CuO embedded silica nanoparticles for tungsten oxidation via a heterogeneous Fenton-like reaction, *Microelectronic Engineering*, 183 (2017) 58–63. <https://doi.org/10.1016/j.mee.2017.10.004>
- Kosmulski M., Compilation of PZC and IEP of sparingly soluble metal oxides and hydroxides from literature, *Advances in Colloid and Interface Science*, 152 (2009) 14–25. <https://doi.org/10.1016/j.cis.2009.08.003>
- Krishnan M., Nalaskowski J.W., Cook L.M., Chemical mechanical planarization: slurry chemistry, materials, and mechanisms, *Chemical Reviews*, 110 (2010) 178–204. <https://doi.org/10.1021/cr900170z>
- Kwon T.-Y., Ramachandran M., Park J.-G., Scratch formation and its mechanism in chemical mechanical planarization (CMP), *Friction*, 1 (2013) 279–305. <https://doi.org/10.1007/s40544-013-0026-y>
- Lee C.F., The properties of core-shell composite polymer latex.: effect of heating on the morphology and physical properties of PMMA/PS core-shell composite latex and the polymer blends, *Polymer*, 41 (2000) 1337–1344. [https://doi.org/10.1016/s0032-3861\(99\)00281-5](https://doi.org/10.1016/s0032-3861(99)00281-5)
- Lee D., Lee H., Jeong H., Slurry components in metal chemical mechanical planarization (CMP) process: a review, *International Journal of Precision Engineering and Manufacturing*, 17 (2016) 1751–1762. <https://doi.org/10.1007/s12541-016-0201-y>
- Lee H., Kim M., Jeong H., Effect of non-spherical colloidal silica particles on removal rate in oxide CMP, *International Journal of Precision Engineering and Manufacturing*, 16 (2015) 2611–2616. <https://doi.org/10.1007/s12541-015-0334-4>
- Lee K., Seo J., Paik U., 12 - Preparation and characterization of slurry for CMP, in: Babu S. (Ed.) *Advances in Chemical Mechanical Planarization (CMP) (Second Edition)*, Woodhead Publishing, 2022, pp. 323–354, ISBN: 978-0-12-821791-7. <https://doi.org/10.1016/B978-0-12-821791-7.00005-8>
- Lei H., Jiang L., Chen R., Preparation of copper-incorporated mesoporous alumina abrasive and its CMP behavior on hard disk substrate, *Powder Technology*, 219 (2012) 99–104. <https://doi.org/10.1016/j.powtec.2011.12.022>
- Lei H., Liu T., Xu L., Synthesis of Sm-doped colloidal SiO₂ composite abrasives and their chemical mechanical polishing performances on sapphire substrates, *Materials Chemistry and Physics*, 237 (2019) 121819. <https://doi.org/10.1016/j.matchemphys.2019.121819>
- Lei H., Zhang P., Preparation of alumina/silica core-shell abrasives and their CMP behavior, *Applied Surface Science*, 253 (2007) 8754–8761. <https://doi.org/10.1016/j.apsusc.2007.04.079>
- Li H., Chen X., Shen D., Wu F., Pleixats R., Pan J., Functionalized silica nanoparticles: classification, synthetic approaches and recent advances in adsorption applications, *Nanoscale*, 13 (2021) 15998–16016. <https://doi.org/10.1039/d1nr04048k>
- Li S., Gaudet G., Sun F., Naman A., ILD CMP with silica abrasive particles: interfacial removal kinetics and effect of pad surface textures, *Journal of the Electrochemical Society*, 157 (2010) H1061. <https://doi.org/10.1149/1.3486806>
- Lim J.-H., Park J.-H., Park J.-G., Effect of iron(III) nitrate concentration on tungsten chemical-mechanical-planarization performance, *Applied Surface Science*, 282 (2013) 512–517. <https://doi.org/10.1016/j.apsusc.2013.06.003>
- Liu C.C., Maciel G.E., The fumed silica surface: a study by NMR, *Journal of the American Chemical Society*, 118 (1996) 5103–5119. <https://doi.org/10.1021/ja954120w>
- Liu T., Lei H., Nd³⁺-doped colloidal SiO₂ composite abrasives: synthesis and the effects on chemical mechanical polishing (CMP) performances of sapphire wafers, *Applied Surface Science*, 413 (2017) 16–26. <https://doi.org/10.1016/j.apsusc.2017.03.270>
- Lu Y.-W., Shie B., Hsiao S., Yang H., Lee S., CMP filter characterization with leading slurry particles, *ICPT 2013, Taiwan*, (2013), <<https://www.entegris.com/content/dam/product-assets/planargardnmbfilter/appnote-cmp-slurry-particles-7561.pdf>> accessed 08.11.2023.
- Lunardi C.N., Gomes A.J., Rocha F.S., De Tommaso J., Patience G.S., Experimental methods in chemical engineering: zeta potential, *The Canadian Journal of Chemical Engineering*, 99 (2021) 627–639. <https://doi.org/10.1002/cjce.23914>
- Luo J., Dornfeld D.A., Effects of abrasive size distribution in chemical mechanical planarization: modeling and verification, *IEEE Transactions on Semiconductor Manufacturing*, 16 (2003) 469–476. <https://doi.org/10.1109/tsm.2003.815199>
- Ma J., Guo X., Ge H., Tian G., Zhang Q., Seed-mediated photodeposition route to Ag-decorated SiO₂@ TiO₂ microspheres with ideal core-shell structure and enhanced photocatalytic activity, *Applied Surface Science*, 434 (2018) 1007–1014. <https://doi.org/10.1016/j.apsusc.2017.11.020>
- Ma P., Lei H., Chen R., Preparation of cobalt-doped colloidal silica abrasives and their chemical mechanical polishing performances on sapphire, *Micro & Nano Letters*, 10 (2015) 657–661. <https://doi.org/10.1049/mnl.2015.0292>
- Margenau H., Van der waals forces, *Reviews of Modern Physics*, 11 (1939) 1–35. <https://doi.org/10.1103/revmodphys.11.1>
- Meled A., Optimization of Polishing Kinematics and Consumables during Chemical Mechanical Planarization Processes, doctoral dissertation, The University of Arizona, 2011, <http://hdl.handle.net/10150/145385>

- Mikhaylichenko K., Post CMP cleans evolution and defect improvement approaches, Business of Cleans / SPCC Conference, 2018, <<https://www.linx-consulting.com/wp-content/uploads/2018/04/Post-CMP-Cleans-Evolution-and-Defect-Improvement-Approaches-SPCC-2018-presented.pdf>> accessed 08.11.2023.
- Moore T.L., Rodriguez-Lorenzo L., Hirsch V., Balog S., Urban D., Jud C., Rothen-Rutishauser B., Lattuada M., Petri-Fink A., Nanoparticle colloidal stability in cell culture media and impact on cellular interactions, *Chemical Society Reviews*, 44 (2015) 6287–6305. <https://doi.org/10.1039/C4CS00487F>
- Mu W., Fu M., Synthesis of non-rigid core-shell structured PS/SiO₂ composite abrasives and their oxide CMP performance, *Microelectronic Engineering*, 96 (2012) 51–55. <https://doi.org/10.1016/j.mee.2012.02.047>
- Nasab M.J., Kiasat A.R., Multifunctional Fe₃O₄@nSiO₂/Pr-Im-NH₂-Ag core-shell microspheres as highly efficient catalysts in the aqueous reduction of nitroarenes: improved catalytic activity and facile catalyst recovery, *RSC Advances*, 6 (2016) 41871–41877. <https://doi.org/10.1039/C6RA00120C>
- Nayl A., Abd-Elhamid A., Aly A.A., Bräse S., Recent progress in the applications of silica-based nanoparticles, *RSC Advances*, 12 (2022) 13706–13726. <https://doi.org/10.1039/d2ra01587k>
- Niibori Y., Kunita M., Tochiyama O., Chida T., Dissolution rates of amorphous silica in highly alkaline solution, *Journal of Nuclear Science and Technology*, 37 (2000) 349–357. <https://doi.org/10.1080/18811248.2000.9714905>
- Ninham B.W., On progress in forces since the DLVO theory, *Advances in Colloid and Interface Science*, 83 (1999) 1–17. [https://doi.org/10.1016/S0001-8686\(99\)00008-1](https://doi.org/10.1016/S0001-8686(99)00008-1)
- Nowatzki P.J., Franck C., Maskarinec S.A., Ravichandran G., Tirrell D.A., Mechanically tunable thin films of photosensitive artificial proteins: preparation and characterization by nanoindentation, *Macromolecules*, 41 (2008) 1839–1845. <https://doi.org/10.1021/ma071717a>
- Paik U., Park J.-G., Nanoparticle engineering for chemical-mechanical planarization: fabrication of next-generation nanodevices, Taylor & Francis, 2009, ISBN: 1420059114. <https://doi.org/10.1201/9780429291890>
- Pan K., Zeng X., Li H., Lai X., Synthesis of silane oligomers containing vinyl and epoxy group for improving the adhesion of addition-cure silicone encapsulant, *Journal of Adhesion Science and Technology*, 30 (2016) 1131–1142. <https://doi.org/10.1080/01694243.2016.1142806>
- Parker J., Next-generation abrasive particles for CMP, *Solid State Technology*, 47 (2004) 30–32.
- Passeri D., Alippi A., Bettucci A., Rossi M., Tamburri E., Terranova M., Indentation modulus and hardness of polyaniline thin films by atomic force microscopy, *Synthetic Metals*, 161 (2011) 7–12. <https://doi.org/10.1016/j.synthmet.2010.10.027>
- Plumeré N., Ruff A., Speiser B., Feldmann V., Mayer H.A., Stöber silica particles as basis for redox modifications: particle shape, size, polydispersity, and porosity, *Journal of Colloid and Interface Science*, 368 (2012) 208–219. <https://doi.org/10.1016/j.jcis.2011.10.070>
- Ralston J., Larson I., Rutland M.W., Feiler A.A., Kleijn M., Atomic force microscopy and direct surface force measurements (IUPAC Technical Report), *Pure and Applied Chemistry*, 77 (2005) 2149–2170. <https://doi.org/10.1515/iupac.77.0089>
- Saka N., Eusner T., Chun J.-H., Nano-scale scratching in chemical-mechanical polishing, *CIRP Annals*, 57 (2008) 341–344. <https://doi.org/10.1016/j.cirp.2008.03.098>
- Sedev R., Exerowa D., DLVO and non-DLVO surface forces in foam films from amphiphilic block copolymers, *Advances in Colloid and Interface Science*, 83 (1999) 111–136. [https://doi.org/10.1016/S0001-8686\(99\)00007-X](https://doi.org/10.1016/S0001-8686(99)00007-X)
- Seipenbusch M., Rothenbacher S., Kirchhoff M., Schmid H.-J., Kasper G., Weber A., Interparticle forces in silica nanoparticle agglomerates, *Journal of Nanoparticle Research*, 12 (2010) 2037–2044. <https://doi.org/10.1007/s11051-009-9760-5>
- Selvarajan V., Obuobi S., Ee P., Silica nanoparticles—a versatile tool for the treatment of bacterial infections, *Frontiers in Chemistry*, 8 (2020) 602. <https://doi.org/10.3389/fchem.2020.00602>
- Seo J., A review on chemical and mechanical phenomena at the wafer interface during chemical mechanical planarization, *Journal of Materials Research*, 36 (2021) 235–257. <https://doi.org/10.1557/s43578-020-00060-x>
- Seo J., Kim J.H., Lee M., Moon J., Yi D.K., Paik U., Size-dependent interactions of silica nanoparticles with a flat silica surface, *Journal of Colloid and Interface Science*, 483 (2016a) 177–184. <https://doi.org/10.1016/j.jcis.2016.08.041>
- Seo J., Moon J., Kim K., Kim Y., Kim S., Paik U., Role of surface chemistry of ceria nanoparticles in CMP, *ECS Meeting Abstracts*, MA2014-01 (2014) 1425. <https://doi.org/10.1149/MA2014-01/38/1425>
- Seo J., Moon J., Kim Y., Kim K., Lee K., Cho Y., Lee D.-H., Paik U., Communication—synergistic effect of mixed particle size on W CMP process: optimization using experimental design, *ECS Journal of Solid State Science and Technology*, 6 (2016b) P42. <https://doi.org/10.1149/2.0171701jss>
- Serrano-Lotina A., Portela R., Baeza P., Alcolea-Rodríguez V., Villarroel M., Ávila P., Zeta potential as a tool for functional materials development, *Catalysis Today*, 423 (2023) 113862. <https://doi.org/10.1016/j.cattod.2022.08.004>
- Shin C., Choi J., Kwak D., Kim J., Yang J., Chae S.-k., Kim T., Evaluation of size distribution measurement methods for sub-100 nm colloidal silica nanoparticles and its application to CMP Slurry, *ECS Journal of Solid State Science and Technology*, 8 (2019) P3195. <https://doi.org/10.1149/2.0261905jss>
- Shluger A., Rohl A., Gay D., Williams R., Atomistic theory of the interaction between AFM tips and ionic surfaces, *Journal of Physics: Condensed Matter*, 6 (1994) 1825. https://doi.org/10.1007/978-94-011-0049-6_17
- Soh S.-Y., Han K.-D., Won H.-Y., Chun Y.-J., Lee B.-J., Yang H.-S., Tetramethyl orthosilicate (TMOS) synthesis by the copper-catalyzed reaction of the metallic silicon with methanol (i)-effect of the manufacturing condition and the composition of contact mass on TMOS synthesis, *Applied Chemistry for Engineering*, 10 (1999) 252–258.
- Song J., Tranchida D., Vancso G.J., Contact mechanics of UV/ozone-treated PDMS by AFM and JKR testing: mechanical performance from nano-to micrometer length scales, *Macromolecules*, 41 (2008) 6757–6762. <https://doi.org/10.1021/ma800536y>
- Srinivasan R., Dandu P.V., Babu S., Shallow trench isolation chemical mechanical planarization: a review, *ECS Journal of Solid State Science and Technology*, 4 (2015) P5029. <https://doi.org/10.1149/2.0071511jss>
- Srinivasan S., Datye A., Smith M., Peden C.H., Interaction of titanium isopropoxide with surface hydroxyls on silica, *Journal of Catalysis*, 145 (1994) 565–573. <https://doi.org/10.1006/jcat.1994.1068>
- Stöber W., Fink A., Bohn E., Controlled growth of monodisperse silica spheres in the micron size range, *Journal of Colloid and Interface Science*, 26 (1968) 62–69. [https://doi.org/10.1016/0021-9797\(68\)90272-5](https://doi.org/10.1016/0021-9797(68)90272-5)
- Sui T., Song B., Wen Y.-h., Zhang F., Bifunctional hairy silica nanoparticles as high-performance additives for lubricant, *Scientific Reports*, 6 (2016) 22696. <https://doi.org/10.1038/srep22696>
- Sun S., Lee K., Lee G., Kim Y., Kim S., Hwang J., Kong H., Chung K.Y., Ali G., Song T., Fe-substituted silica via lattice dissolution–reprecipitation replacement for tungsten chemical mechanical planarization, *Journal of Industrial and Engineering Chemistry*, 111 (2022) 219–225. <https://doi.org/10.1016/j.jiec.2022.04.001>
- Szekeres M., Kamalin O., Schoonheydt R.A., Wostyn K., Clays K., Persoons A., Dékány I., Ordering and optical properties of monolayers and multilayers of silica spheres deposited by the Langmuir–Blodgett method, *Journal of Materials Chemistry*, 12 (2002) 3268–3274. <https://doi.org/10.1039/b204687c>
- Tamboli D., Seal S., Desai V., Maury A., Studies on passivation behavior of tungsten in application to chemical mechanical polishing, *Journal of Vacuum Science & Technology A: Vacuum, Surfaces, and Films*, 17 (1999) 1168–1173. <https://doi.org/10.1116/1.581790>
- Tao C., Li J., Zhang Y., Liew K.Y., Effect of isomorphic substitution of zirconium on mesoporous silica as support for cobalt Fischer–

- Tropsch synthesis catalysts, *Journal of Molecular Catalysis A: Chemical*, 331 (2010) 50–57.
<https://doi.org/10.1016/j.molcata.2010.08.002>
- Tolias P., Lifshitz calculations of Hamaker constants for fusion relevant materials, *Fusion Engineering and Design*, 133 (2018) 110–116.
<https://doi.org/10.1016/j.fusengdes.2018.06.002>
- van Oss C.J., Chapter three - the extended DLVO theory, in: van Oss C.J. (Ed.) *Interface Science and Technology*, Vol. 16: The Properties of Water and their Role in Colloidal and Biological Systems, Elsevier, ISBN: 9780123743039, 2008, pp. 31–48.
[https://doi.org/10.1016/S1573-4285\(08\)00203-2](https://doi.org/10.1016/S1573-4285(08)00203-2)
- Wang C.-X., Zhang X.-F., A non-particle and fluorine-free superhydrophobic surface based on one-step electrodeposition of dodecyltrimethoxysilane on mild steel for corrosion protection, *Corrosion Science*, 163 (2020) 108284.
<https://doi.org/10.1016/j.corsci.2019.108284>
- Wang F., Pi J., Li J.-Y., Song F., Feng R., Wang X.-L., Wang Y.-Z., Highly-efficient separation of oil and water enabled by a silica nanoparticle coating with pH-triggered tunable surface wettability, *Journal of Colloid and Interface Science*, 557 (2019) 65–75.
<https://doi.org/10.1016/j.jcis.2019.08.114>
- Wang J., Wang T., Pan G., Lu X., Effect of photocatalytic oxidation technology on GaN CMP, *Applied Surface Science*, 361 (2016) 18–24.
<https://doi.org/10.1016/j.apsusc.2015.11.062>
- Wang W., Zhang B., Shi Y., Ma T., Zhou J., Wang R., Wang H., Zeng N., Improvement in chemical mechanical polishing of 4H-SiC wafer by activating persulfate through the synergistic effect of UV and TiO₂, *Journal of Materials Processing Technology*, 295 (2021) 117150.
<https://doi.org/10.1016/j.jmatprotec.2021.117150>
- Wang W., Zhang B., Shi Y., Zhou D., Wang R., Improvement in dispersion stability of alumina suspensions and corresponding chemical mechanical polishing performance, *Applied Surface Science*, 597 (2022) 153703. <https://doi.org/10.1016/j.apsusc.2022.153703>
- Wells J., Koopal L., de Keizer A.d., Monodisperse, nonporous, spherical silica particles, *Colloids and Surfaces A: Physicochemical and Engineering Aspects*, 166 (2000) 171–176.
[https://doi.org/10.1016/S0927-7757\(99\)00462-8](https://doi.org/10.1016/S0927-7757(99)00462-8)
- Xu B., Dong L., Chen Y., Influence of CuO loading on dispersion and reduction behavior of CuO/TiO₂ (anatase) system, *Journal of the Chemical Society, Faraday Transactions*, 94 (1998) 1905–1909.
<https://doi.org/10.1039/a801603h>
- Xu D., Cheng F., Lu Q., Dai P., Microwave enhanced catalytic degradation of methyl orange in aqueous solution over CuO/CeO₂ catalyst in the absence and presence of H₂O₂, *Industrial & Engineering Chemistry Research*, 53 (2014) 2625–2632.
<https://doi.org/10.1021/ie4033022>
- Zhang B., Lei H., Chen Y., Preparation of Ag₂O modified silica abrasives and their chemical mechanical polishing performances on sapphire, *Friction*, 5 (2017) 429–436.
<https://doi.org/10.1007/s40544-017-0156-8>
- Zhang X., Pan G., Wang W., Guo D., Polishing behavior of PS/SiO₂ Core-Shell nanoparticles with different shell thickness on fused silica Chemical Mechanical Polishing, *IOP Conference Series: Materials Science and Engineering*, 563 (2019) 022048.
<https://doi.org/10.1088/1757-899X/563/2/022048>
- Zwicker G., 19 - Applications of chemical mechanical planarization (CMP) to More than Moore devices, in: Babu S. (Ed.), *Advances in Chemical Mechanical Planarization (CMP)* (Second Edition), Woodhead Publishing, ISBN: 9780128217917, 2022, pp. 533–557.
<https://doi.org/10.1016/B978-0-12-821791-7.00001-0>

Authors' Short Biographies



Ganggyu Lee received his B.S. degree from the Department of Energy Engineering at Hanyang University, South Korea, in 2020. He is currently a Ph.D. candidate in Prof. Ungyu Paik's Nano Device Process Laboratory (NDPL) group at Hanyang University. His research interest mainly focuses on colloid chemistry and the semiconductor manufacturing process, including chemical mechanical polishing.



Kangchun Lee received his Ph.D. degree from the Department of Energy Engineering at Hanyang University, South Korea, in 2020. Now, he has been an Assistant Professor in the Department of Electronic Engineering at Kyonggi University, since 2023. Prior to joining Kyonggi University, he was a Staff Engineer at the Semiconductor R&D Center in Samsung Electronics, from 2020 to 2023. His research focuses on Advanced CMP/Post-Cleaning Processes and cutting-edge materials based on Colloid- and Electrochemistry.



Seho Sun received his Ph.D. degree from the Department of Energy Engineering, Hanyang University, South Korea, in 2022. He worked as a senior research engineer at Samsung Electronics from August 2022 to August 2023. Since September 2023, he has been an Assistant Professor at the School of Chemical Engineering in Yeungnam University. His current research focuses on semiconductors, energy storage, and electro catalysis.



Taeseup Song received his Ph.D. degree from the Department of Materials Science and Engineering at Hanyang University, South Korea, in 2012. He is currently an Associate Professor of the Department of Energy Engineering at Hanyang University. His research interest mainly focuses on synthesizing nano-structured materials for energy and electronic applications.



Ungyu Paik is a Distinguished Professor of the Department of Energy Engineering at Hanyang University, South Korea. He received his Ph.D. degree from the Department of Ceramic Engineering at Clemson University in 1991. His research interest is the synthesis and engineering of nanomaterials for applications in energy and electronic devices.